Vilniaus universiteto
Fizikos fakulteto

Lazerių tyrimų centras

Marius Lazdauskas

Specialų keramikų paviršiaus ženklinimas femtosekundiniais impulsais sukūriant didelio kontrasto, hidrofobiškus raštus.

Magistrantūros studijų baigiamasis darbas

Lazerinės technologijos

Magistrinių studijų programa

Studentas   Marius Lazdauskas

Leista ginti   2021-05-21
Darbo vadovas   prof. habil. dr. Valdas Sirutkaitis
Konsultantas   dr. Simas Butkus

Instituto/Centro direktorius/atstovas   prof. dr. Aidas Matijošius

Vilnius 2021

Vilnius University

Faculty of physics

Laser Research Center

Marius Lazdauskas

Marking of hydrophobic high contrast patterns on surface of special ceramics with
femtosecond laser pulses

Master's final work

Laser technology studies program

Student   Marius Lazdauskas

Allowed to defend   2021-05-21

Supervisor   prof. habil. dr. Valdas Sirutkaitis
Consultant   dr. Simas Butkus

Director of LRC   prod. dr. Aidas Matijošius

Vilnius 2021

1

Content

Introduction.

Laser marking is most applied and developed marking technology for its ability to mark any kind of material and create permanent marks. In this work special laser marking with ultrashort laser pulses at different harmonics was applied for glass ceramic material. Ceramic material used in this work is very brittle, hard, dark brown color with good thermal stability and low thermal conductivity, high chemical resistance and it is widely used in home appliances, mostly for induction cooktops. Ultrashort pulses generates high peak power which causes nonlinear absorption and affects precisely required area. In this work CARBIDE laser, which can generate ultrashort pulses with tunable duration in range from 243 fs up to 10 ps was used. Also this laser had tunable repetition rate from 60 kHz up to 600 kHz and tunable power. By variating laser parameters, scanning patterns and speed main task for this work was to create high contrast hydrophobic patterns. Glass ceramic material is relatively unresearched material type in laser marking. There are not many research made with this type of glass ceramic material, no examples of textured and manufactured hydrophobic high contrast marks made on glass ceramics. As glass ceramic from itself is hydrophilic material, created marks also tends to be hydrophilic so water and dirt accumulates on the mark, contrast of the mark decreases and fades over time. Hydrophobic surface would solve this problem and would give self-cleaning abilities to the mark.

1. Laser marking process introduction.

Laser system is one of the most innovative ways to process materials nowadays. Lasers are used in many ways: material cutting, marking, drilling, soldering, coding, medicine, material research, biological research. Laser marking is one of the well-developed technologies of materials processing. It is the best and most applied permanent marking method. Most popular laser for marking are CO_2 pulsed lasers, pulsed solid-state lasers (for example Nd:YAG) and pulsed fiber lasers (mainly doped with Yb), excimer lasers which are also pulsed by nature. CO_2 lasers generally are more appropriate for marking of plastics, paper, wood. Excimer lasers are used for high precision marking and also on brittle materials, ceramics, glasses or materials which have high absorbance in ultraviolet range. Pulsed fiber and solid-state lasers are more used on metals and alloys. Through generation of higher harmonics pulsed fiber and solid-state lasers are able to generate wavelengths from infrared to ultraviolet spectrum. In laser marking system beam trajectory can be controlled using computer-controlled mirrors and scanners or using a fiber and the workpiece can be moved using X-Y-Z axis table. Laser marking has many advantages such as no pollution, high speed, high quality and precision, flexibility, and do not contact the workpiece compared with traditional electrochemical or machinery marking method, have long maintenance intervals (10000-14000 hours), easy to integrate. Those advantages make laser marking technology appear in wide area of industry and it is one of the most popular way to use lasers [1-3].

In 2019 laser market revenue reached \$2.1B and it is predictable that in 2024 laser marking market will reach \$3B [4]. In Table 1 is noticeable that laser marking compared with other marking methods and processes excels at speed, mark durability, image flexibility contrast and have good reliability. Laser marking has great potential in diverse range of applications: electronic components, automotive products, jewelry, medical implants, surgical instruments, surfaces of household appliances. All sort of materials can be processed if we have compatible laser for marking of that material including metals, ceramics, glass, wood, leather [3, 5, 6].

Marking process	Speed	Durability	Image flexibility	Contrast
Laser marking	Good	Good	Good	Good
Chemical etch	Good	Good	Poor	Poor
Photo etch	Good	Good	Poor	-
Ink jet	Good	Poor	Good	Moderate
Mechanical stamping	Good	Good	Poor	Poor
Nameplates	N/N	Moderate	Poor	Good
Casting/molding	Good	Good	Poor	Poor
Pneumatic pin	Moderate	Good	Moderate	Poor
Vibratory pencil	Poor	Good	Good	Poor
CO_2 mask marker	Good	Moderate	Poor	Moderate

Table 1. Comparison chart of marking techniques [6].

Laser marking also has disadvantages and new problems occurs when technology improves. First of all laser marking systems is a very high investment. Some lasers can mark only certain materials and every laser have it's own disadvantages and limits. Also it requires high-quality workers to work with laser, not all laser can work with low ignition point materials. Laser

marking technique mostly depends on heating, melting and vaporization so it always damages material and can cause unnecessary chemical reactions, can change marked spot material properties, for example, in this work used glass-ceramic material marked area becomes hydrophilic. So with every material you have to precisely adjust laser parameters to get good contrast and required color and properties. Sometimes even laser properties could not get required color on the material, so some material gets specially prepared or doped [7].

1.1. Laser marking methods and mechanisms.

Laser marks are created by vaporizing, melting or annealing the material and making surface modifications. Each of the processes have certain effect for different material. Figure 1 shows that a lot physical and chemical processes can have an impact when you mark the material in this example on the metals. When laser beam is focused on the surface of the material, the thermal energy is absorbed which creates new charges or make material lattice to vibrate and oscillate. These processes create heat, new chemical reactions appears. Heating caused by thermo and photo structural changes cause material to melt and vaporize or react with oxygen and other elements in the air [3, 7]. Chemical reactions occurs because material gets energy to create new free charges in the material, so material can interact also with the air, bond with other elements or dopants in the material, change lattice structure [7, 8].

Fig. 1. Physical processes in laser marking. [3]

Examples of marking are shown in Table 2. When marking with the right parameters of the laser we can get good contrast of color even if we affected very small area and depth of the material. That's why laser marking specifies precise demands of marking [9].
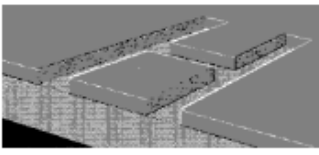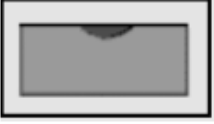
Process	Schema		Mechanism
Vaporization			Material removal mainly by vaporization
Thin layers material removal			Thin layers material removal by controlled vaporisation, changing the colour of the under layers
Carbonisation or coloration			Colour changing by photo-thermal or photo-chemical reactions
Surface modify by material fusion			Destruction of materials by pyrolyze reaction that leads to irregular structures into the material

Table 2. Several examples of marking [9].

Mechanisms for marking can be divided by removing material from surface or making surface modifications. In this work we were using marking mechanisms which removes material form the surface [10]. So mainly marked are parameters, contrast and color depend on marking process, material and laser parameters.

1.2. Removal from surfaces laser marking techniques.

Laser marking creates visible marks by melting, vaporizing, ablating or engraving. It also results surface morphology but creates high contrast marks. Main removal from surfaces methods: laser etching, surface melting, ablation, engraving [9].

Laser etching is a process when heat applied to material causes substrate surface melting. Laser beam heats the surface of the material and after the action material cools off and changes affected area changes. This process removes small amount of material to create a mark. This excitation action caused by absorption of the material and liquid or gas around the component, depending of the wavelength, absorption causes electronic excitation, phonon vibrations material melts and heats. This method is beneficial because input energy required to initiate this action is relatively small, so thermal loading on the material is minimized, also very small are gets affected to get excellent results. This method causes less damage on the surface and marked area cannot be remove by rubbing surface with fingers. In Dahotre and Harimkar book excellent result obtained when component was penetrated less than 25 μm [10]. However etching causes cracks in processed material and high temperature reaches parts and spreads through material, causes additional stress in materials volume [5].

In surface melting method usually laser beam removes a layer of coating to reveal base material. The surface can be plotted with special foil, films, anodized metals or metal oxide. Surface melting creates detailed very sharp graphics and high contrast between coating and base material. With this marking method you can also get good results at penetration depths less than 25 µm. This method doesn't require high energy, because it can cause explosive ablation on the thing films. Surface melting usually used in plastics and on this work we mainly focusing on ceramic and glass materials [5].

In engraving method laser beam penetrates the surface and removes the material in laser path by melting and evaporating it. This method involves more heat than laser etching and results removal of working piece. Once material resolidified, modified structure occurs in the changed form. This method does not create high contrast and usually pulsed lasers are used in this method, but it causes less damage to the substrate and causes less stress to the material and cracking. This method can't work with materials thinner than 2.5 mm, but it's beneficial that nearly any material can be engraved. Laser engraved parts are very durable and can only be removed by grinding [5, 11].

In ablation high intensity laser pulse interacts with material, usually this process performed in vacuum or air. Heat increases through absorption of laser beam and it depends on material conductivity and thermal capacity, absorbance light spectrum. Vaporization appears when temperature reaches melting temperature threshold. In ablation material have to reach high temperatures instantly otherwise vapor can cause injection of melt and create additional debris around affected area. Debris and recast can create inhomogeneous surface which affects precision and marks visibility. They can be minimized by choosing right parameters of laser system. Generally, shorter pulses are more efficient and produce less unwanted depositions near the processing are also peak beam intensity also increases. In this process material removed from work peace result change in coloration. There are a lot of parameters which can make different results of the marking including laser parameters and also ablated material type [2, 5, 7].

2. Laser marking process parameters.

When selecting marking system there are many factors to consider: power density, wavelength, pulsed or continuous laser, beam quality specifications if laser is pulsed repetition rate is also important, scanning speed, focused spot size. In this work pulsed laser were used so mainly parameters to look after when you work with this type of lasers are wavelength, average laser power, quality of the beam, pulse repetition rate, maximum energy per pulse, pulse duration [2]. To get good color contrast, precise results and microstructured mark you have to selected laser parameters precisely, because every parameter can have an impact what color and contrast you will get, how deep material will be ablated and affected by laser [5, 9].

2.1. Pulse frequency and scanning speed.

The pulse repetition rate determines the amount of time between laser pulses allowed to strike the surface. The high peak power pulses at low repetition rate will rapidly increase surface temperature resulting instant vaporization and minimal heat conduction of the affected area. At higher repetition rates, lower peak power will be produced, but it will create more heat in the material. It's important to have required pulse repetition rate for each material, for example in plastics smaller volume of peak power is required and more heat generates other processes which can make material to change it properties. For metals and ceramics higher pulse energy is required for material vaporization and melting. Pulse repetition rate can have an impact of incubation and energy accumulation in the material where M. Kumkar, L.Bauer shown in their work (Fig 2.). Although in their work on lower repetition rate (10 kHz) material was already damaged, but in higher repetition rate (20 kHz) material didn't get damaged but affected zone in the glass was larger. Biggest energy accumulation and damage was reached with highest tested repetition rate (200 kHz) where it's seen that damage region is much larger, heat accumulated area is much bigger, noticeable microcracks appeared [14]. So when you change pulse repetition rate but maintain same pulse energy, pulse repetition frequency can have a big impact on damaged material morphology, damage type and volume.
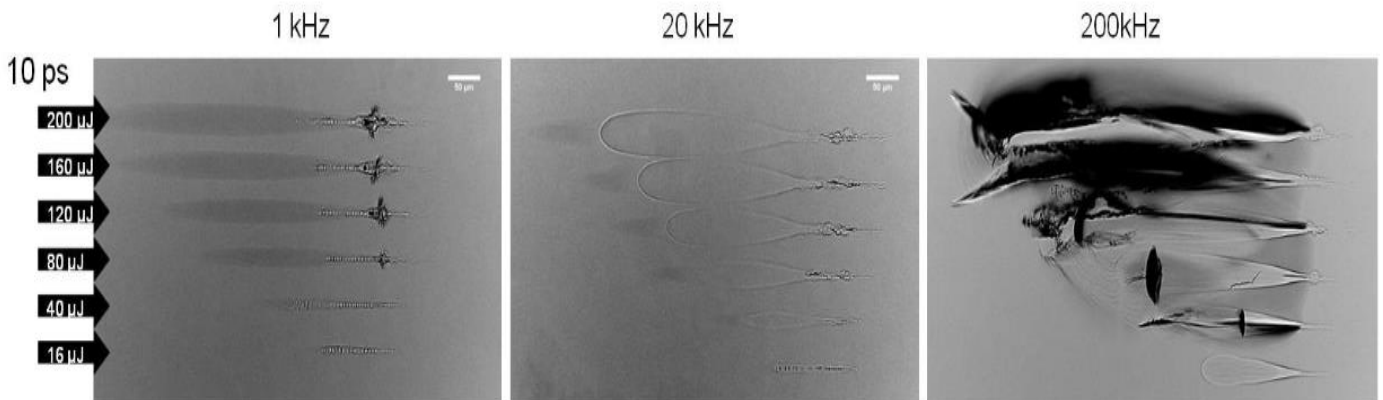

Figure 2: Modifications inside glass (hardened Corning Gorilla®) by 32 pulses of 1 ps duration at different repetition rates. Rayleigh length of focused beam was 38 μm in air [14].

Pulse frequency are relatable with scanning speed too, at lower scanning speed and higher repetition rate pulses can overlap with each other creating more heat in the material. By controlling pulse frequency and scanning speed marking manufacturers can suggest if they want pulses to overlap or mark material when each pulse hits different location and don't overlap with each other and measuring how much we want different pulses be apart from each other [10]. M. Sun with the team in their article had investigated and researched how damage mechanisms depend from spatial overlap of the ultrashort pulses (50 fs). They measured how damage region and depth changes when pulses overlap between each other 0%, 54%, 85% 90% when pulse energy remains almost the same (from 40 μJ to 50 μJ). In the Figure 3 we can see the results of the damaged area from which researchers noticed that in with the overlaps of 0% (a) example) and 54% (b) example there is some irregular dark spikes which indicates that the electronic damage was dominant. In the same Figure 2, c) and d) photos shows that laser pulses affected bigger area of the material and smoother contours is seen, this zones is created

by diffusion process because when pulses overlap the energy accumulation becomes significantly higher and heat diffusion leads to heat modified zones. Even though in all examples electronic damage was created but when pulse overlap too much heat caused diffusion damage influence increases and become more dominant. This means when you work with ultrashort pulses scanning speed and pulse frequency can have a big impact on damage mechanism [15].
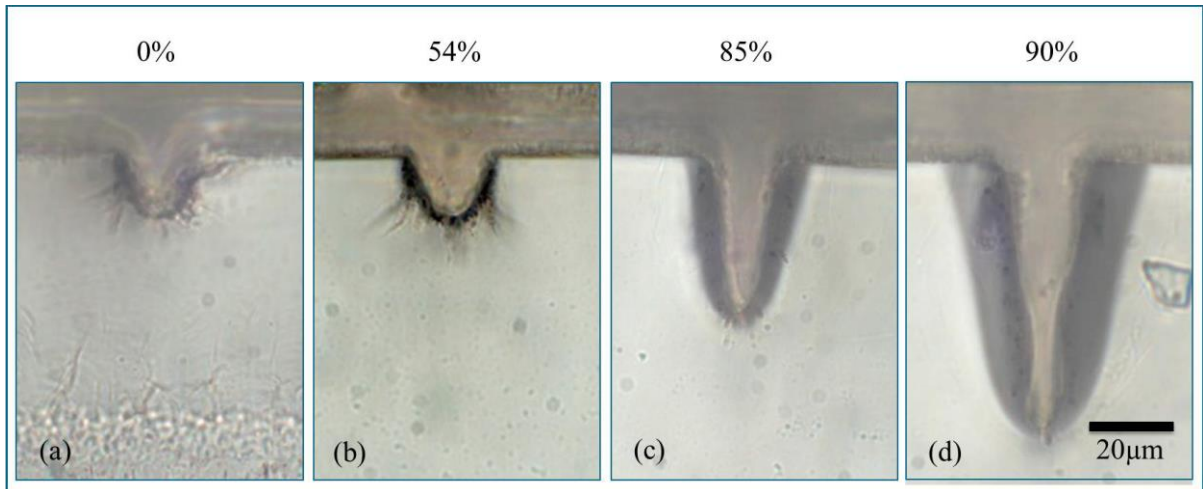

Fig. 3. Cross sections of the damage regions with different spatial overlaps (a) 0%, (b) 54%, (c) 85%, and (d) 90%. The conditions for all the cases are carried out with pulse energy of 40 µJ, except for 54% overlap with 50 µJ, 5 passes, and a repetition rate of 400 kHz [15].

In laser marking scanning speed is important variable in the thermal process and must be calculated to achieve desired process results. For deep marking (>0.05 mm) each point on the marked line will require exposure of several pulses or more so the beam speed must be reduced until desired depth is achieved. For shallow marking scanning speed can be increased to maximum speed until separation between pulses becomes aesthetically unacceptable. If we want to have appearance of continuous mark, pulses should overlap at least 50% and 70-90% to ensure good marking [5, 13].

2.2. Focused spot size and position.

On focal spot maximum energy density is achieved, so focal spot size is very important factor for marking materials. Focal point position on the material also is very important factor which can determine ablated region diameter, shape and depth. S. Campbell in his work were analyzing how focus position can have an impact on hole diameter, damaged area and shape on the BK7 glass. Beam focused above the sample surface (Fig. 4) creates almost round shaped hole and just have slightly increased diameter on vertical axis. Perfect round shape can be only formed when focus is on the surface of the material (Fig. 4). When focus point is inside the sample we can see that damaged area gets wider in horizontal area (Fig. 4) [16].

Fig 4. Damaged shape dependence on focus position. a) Focus point is 200µm above the surface; b) Focus position is on the surface; c) Focus position is 200µm inside the material. Pulse width: 150fs, wavelength 800 nm, repetition rate 5kHz, pulse energy 0.16mJ [16].

Focal point position also has an impact on ablated hole diameter and area. In Fig. 5 it's shown that on lower pulse energies on the surface focused beam creates bigger diameter and area holes. When pulse energy increases an impact of focus position increases, on higher pulse energies holes affected area and diameter gets bigger in the position where focus is above or in the material. It becomes an issue when you need high quality marking and precise formation of microstructures on the surface [16].
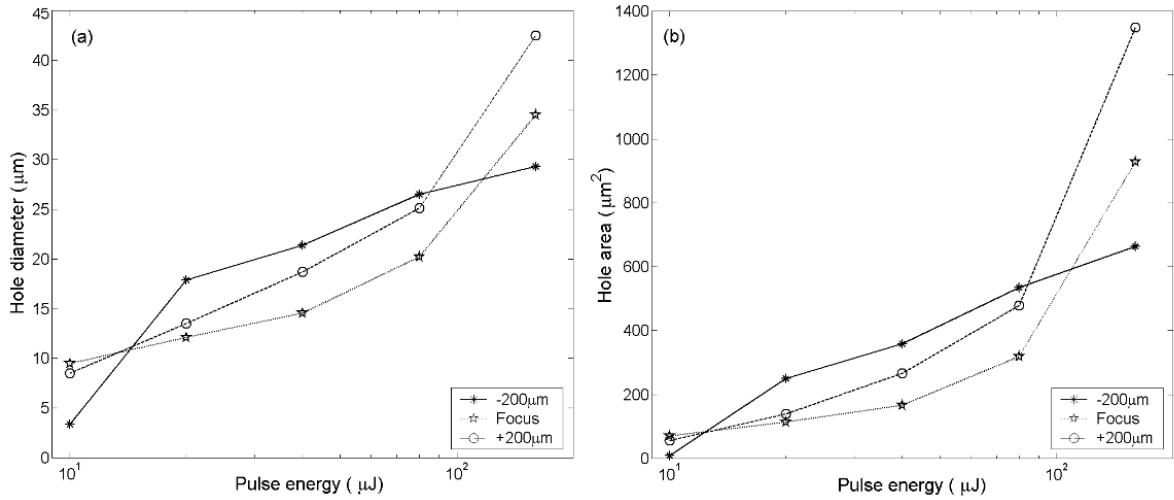
Fig. 5. a) Dependance on hole diameter against pulse energy on three different focal positions; b) Dependance of hole are on three different focal position and pulse energy. Pulse width 150 fs, wavelength 800nm, repetition rate 5kHz [16].

The diameter of the focused laser beam determines marking linewidth and marking efficiency and precision. The spot diameter determined by focal length of a focusing lens divergence of laser beam, laser wavelength. This implies that increasing lenses focal point also determines in increasing of focused laser beams diameter. Focused spot size determines energy density of marking spot and marking field area. Also focused beam size is important for smaller Rayleigh length, which determined by formula (2.2):

$$z_R = (\pi\omega_0^2)/\lambda \qquad (2.2)$$

Where z_R is Rayleigh length, ω_0 – beam waist at narrowest point, λ – wavelength.

Fig. 6 shows how Rayleigh length can affect the length of modification on different pulse energies, respectively 44 µJ and 87 µJ, when Rayleigh length increases modification size also gets larger. On higher energies it has more impact and affected is much bigger compared to lower energies. It is beneficial when you want laser beam to affect bigger area of the material and is mostly used in cutting. In marking Rayleigh length can be a disturbance because it can decrease the quality and precision. When you create hydrophobic surfaces on the ceramic material, it is important affect zones precisely so we can create required patterns [14].
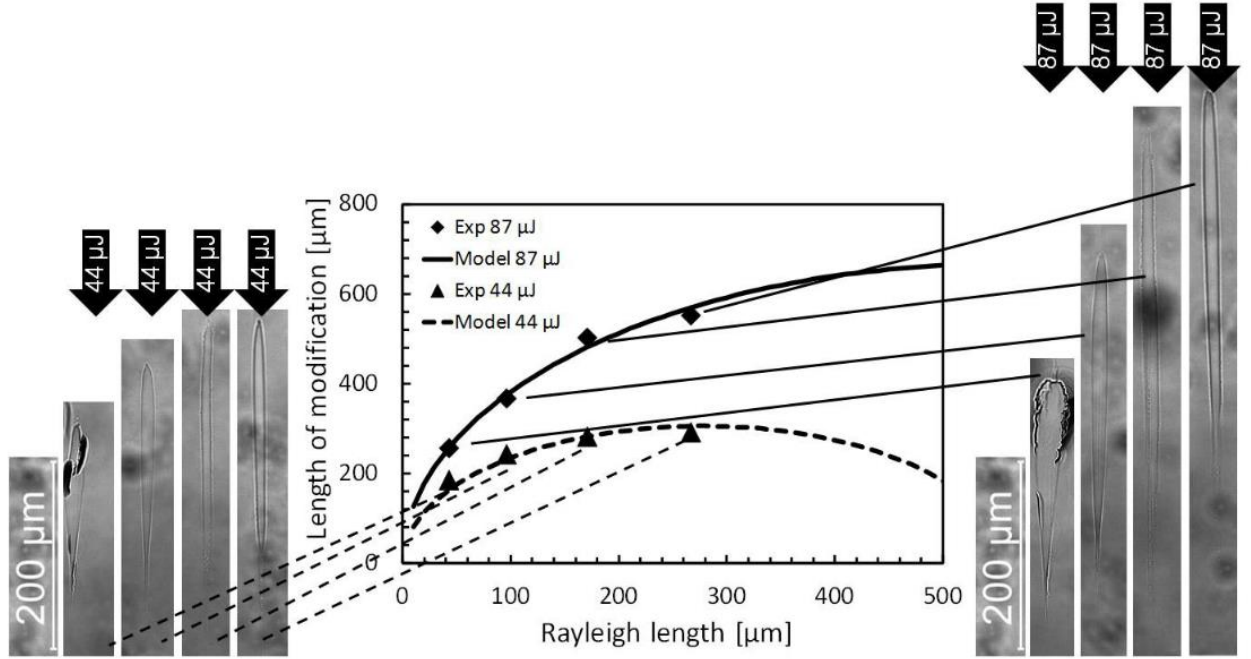

Fig. 6. Length of medication value relation to Rayleigh length. On the sides pictures of affected volume by laser depending on Rayleigh length [14].

The focal point determined by formula (2.2.1):

$$d = (2f\lambda)/D \qquad (2.2.1)$$

Where d is the diameter of focused beam, f is the focal length of the focus lens. D is the entrance beam diameter, and λ is wavelength of laser beam. Also focused spot diameter closely relates with pulse overlapping [10].

2.3. Laser power.

Laser power is one of the most important in laser marking because it directly affects a laser's ability to perform ablation process. Operating mode (pulsed or continuous wave) also affects marking quality, absorption type, vaporizing or melting abilities, marking type, quality and which materials we can manage to mark. For pulsed lasers most important parameter is peak power which depends on lasers repetition rate, power, pulse duration. Output power is closely related with processing time and operation expense. If the selected power is lower, the processing time and speed increases. Too much power can cause increase in expenses. For pulse laser peak usually expressed:

$$P_{peak} = \frac{P_{avg}}{f \times \tau}, \qquad (4)$$

P_{peak} – peak power of the pulse; P_{avg} – average laser power; f – pulse frequency or repetition rate; τ – pulse duration.

For most cases laser marking requires high peak power, especially for ceramics and metals, for pulsed laser it can be achieved by shortening pulse duration or lowering repetition rate. High peak power and shorter impulses leads to smaller heat-affected zones and better mark quality, also to nonlinear absorption appears and sometimes shorter pulses have smaller affect duration on the material so accumulated heat in that period of time can't make any changes in material, especially when material have big thermal conductivity. Fig. 7 shows how laser fluence have an impact on ablation depth on K9 glass [5, 13, 17, 18].
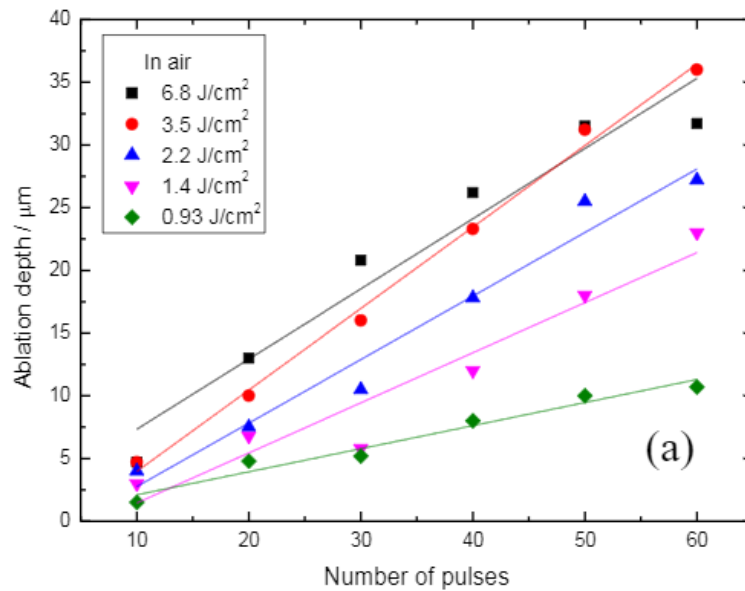

Fig.7. Ablation depth dependance on laser fluence in air environment. Pulse width 50 fs, laser wavelength 800nm [18].

2.5 Pulse duration.

Pulse duration is one of the main factors in the material marking because it's one of the main parameters to describe peak power. Pulse width have a big impact on processes which will appear in the material because laser absorbed energy Q_L can be approximated (2.5.0):

$$Q_L = AP_L t_i \qquad (2.5.0)$$

Where A (%) is the absorptivity of the workpiece, P_L (W) is the laser incident power, t_i (s) is interaction time between laser beam and material [17]. When interaction time with material is longer heat diffusion, melting processes and thermal wave propagates around affected area. When pulse width is shorter interaction time becomes smaller with the material also laser peak power increases thermal wave does not propagates so much and nonlinear processes appears like multiphoton ionization, with high peak power laser beam can instantly vaporize an area creating plasma so affected is smaller (Fig 8 and Fig 9). For example in aluminum heat affected zone was 1.5 µm wide after ablation of 200fs, where heat affected zone using 20 ns laser pulses was 20 µm wide. Ultrashort pulses let create high resolution, precise markings and can mark any material, very thin wafers, films, sheets and surfaces [14, 18 - 21].
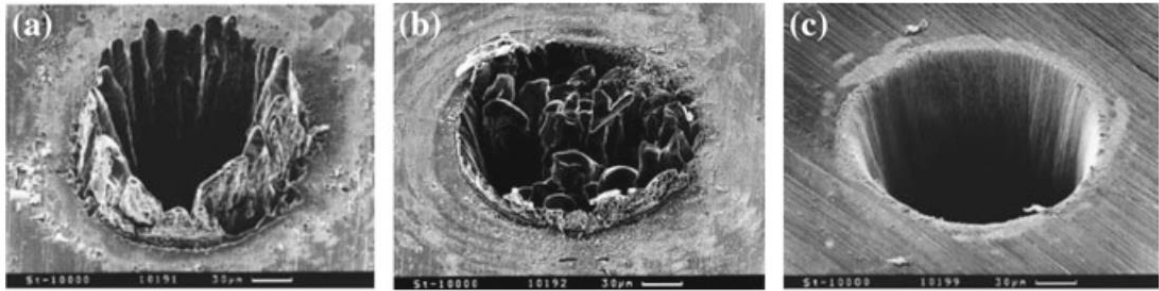
Fig 8. Laser ablated 100 µm craters in steel on vacuum environment (10^{-4} mbar), Laser Ti:Saphire laser. a) Pulse duration: 3.3ns, Laser fluence (4.2 J/cm^2); b) Pulse duration: 3.3ns, Laser fluence (3.7 J/cm^2); c) Pulse duration: 200 fs, Laser fluence (0.5 J/cm^2) [18].
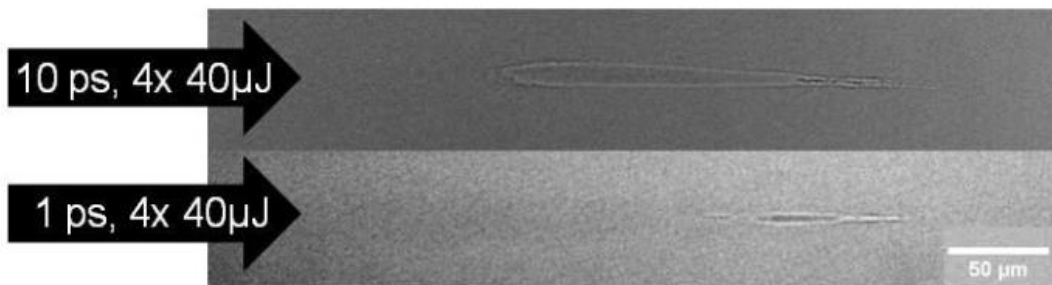

Figure 9: Affected area inside the glass (Corning Gorilla). Glass was affected by four 40 µJ pulses with interval of µs with different pulse duration 10 and 1 ps [19].

W. Kauted, J. Kruger and other in their work researched and experimented how laser pulse duration affects ablation depth, volume, ablation threshold on Barium aluminium borosilicate glass. Pulse number (Fig. 10) don't have a big impact on ablation depth when pulse duration is lower than 100 fs, because heat diffusion gets neglected of the short interaction time with material. For pulses shorter than 100 fs, laser fluence have bigger impact because multiphoton ionization is solely relates on laser fluence. Ablation threshold is lower for shorter pulses, because they have higher peak power (Fig. 10). Comparing ablation threshold from Figure 10 it is noticeable that 20 fs pulses have about 5 times lower ablation threshold than 3 ps pulses. Pulse number have bigger impact on longer pulses as for example in Figure 9 ablation depth have linear increase rate with pulse number. If we compare ablation depth dependance on pulse number between pulse lengths of 20 fs and pulses longer than 100 fs, from example (Fig 10) we can relate that that with higher pulse number ablation depth can have difference up to 4 times. So shorter pulses can let us mark reach lower ablation thresholds and keep good ablation rate and precision, but longer pulses affect material more which can help us to create good contrast in color marking and help us reach good depth for creating microstructures, patterns on the surface [21, 22].
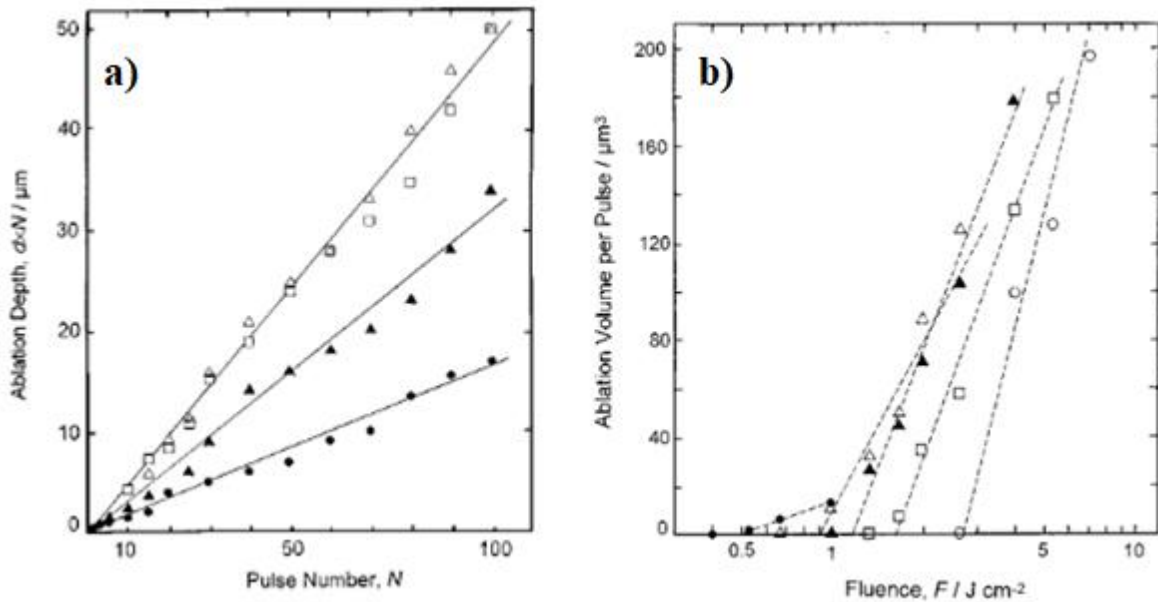
Fig. 10. a) Ablation depth dependance on pulse number at air, pulse energy 60 µJ, d – ablation depth. Pulse durations: ● – 20fs; ▲ – 50 fs; △ - 120 fs ;□- 300 fs. b) Ablation volume per pulse dependance on laser fluence. 50 pulses, Pulse duration: ● – 20fs; ▲ – 50 fs; △ - 120 fs ;□- 300 fs.; ○ – 3000 fs. Λ – 780nm. Material: Barium Borosilicate glass [22].

3. Evaluation of marking quality characteristics.

Laser mark quality characteristics is done by evaluating mark width, depth and intensity, color contrast. The quality characteristics are usually evaluated using complementary techniques such as optical microscopy, surface roughness measurement, contrast evaluation, spectroscopy or contrast evaluation [5].

3.1. Mark width

The width of the line segment which is formed by laser is referred to mark width. Mark width mostly depends and controlled by the focused beam spot size. Other parameters such as beam scanning speed, laser power density and material absorptivity also affect the line width. Mark width simply can be measured by optical microscope [5].

3.2. Mark depth.

Marking depth usually determined by laser power and intensity and the interaction between laser beam and material, materials absorptivity of the laser beam generating wavelength. Marking depth is measured using profile instrument. The depth of marking and penetration can vary from a few microns to several tens of millimeters. The assist of compressed gas enhance the evaporation of material from marking zone which further results in more marking depth, assisting gasses can be oxygen, nitrogen or just air [5].

3.3. Mark intensity.

Mark intensity defined by visible brightness of a certain mark and unmarked portion of the sample. The measurement of marking contrast is done with image analysis software. The sharpness or resolution of the marked edges affects the marking contrast or intensity. Mark intensity is one of the main parameters for marking various appliances and barcodes, writings, poor edge sharpness or small color contrast can cause problems failure for computer readings. Better edge resolution can be produced due to high peak power, small focal spot size, shorter pulses. Contrast can be determined:

$$contrast = \frac{g_{background} - g_{mark}}{g_{white} - g_{black}} \qquad (3.3)$$

Where $g_{backround}$ – grey level value of unmarked area; g_{mark} – grey level of marked area; g_{black} - grey level of black colour and g_{white} – is the grey level of white color. After taking photograph through optical microscope, the images are analyzed in a computer [5, 13].

4. Light scattering from the surface.

Surface is explained to be a structure of periodic peaks and valleys. This explanation applies to characterize roughness, waviness and deviation of the surface. If we would divide surface in particular parts with certain values of S_w (divided length of certain surface part) and W_z (surface height of divided surface part) we can adjust what type of surface we have and ratio S_w/W_z let's us characterize type of the surface. If $1000 \geq S_w/W_z \geq 40$ – it's waviness, $S_w/W_z \geq 1000$ – deviation of surface, $S_w/W_z < 40$ – roughness. And surface roughness has most impact for light diffraction and scattering. To evaluate surface peak to valley values are important, but in this work we will use root mean square values (4.0) [23, 24]:

$$\sigma_{RMS} = \sqrt{\frac{1}{N}\sum_{i=1}^{N} z_i^2}, \qquad (4.0)$$

where N – number of measures, z_i – surface deviation from average roughness.

For light scattering from the surface we can use model of diffraction gratings. It tells that we can look at the surface like it's made from a lot of diffraction gratings. If we could adjust that surface is a sum of different types of diffraction gratings with different angles, periodicity we can adjust that diffracted light depends on the period of the diffraction gratings and not from number of gratings in the 1 mm range (Fig. 11) [24].
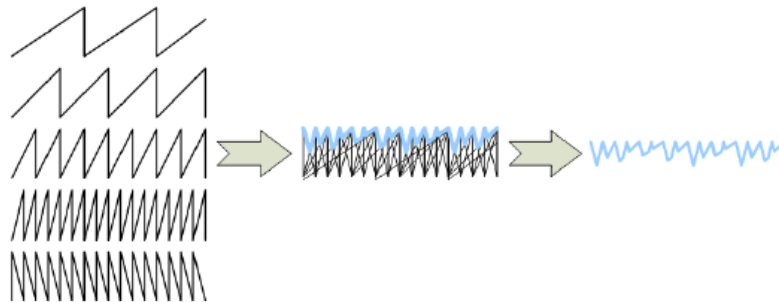

Fig. 11. Visual explanation that surface is made of different diffraction gratings.

Diffraction losses can be approximated:

$$S = \frac{P_s}{P_0},$$ (4.0.1)

where P_s – power of scattered light; P_0 – power of incident light on the surface. From Rayleigh-Rice theory or vector diffraction theory which evaluates and describes scattering angles and properties of scattered light where scattering can be approximated if:

1. Correlation length is much higher than the incident light:

$$S = \left(\frac{4\pi\sigma}{\lambda}\right)^2.$$ (4.0.2)

2. Correlation length τ_c is much lower than the incident light:

$$S = \frac{64}{3}\pi^4 \frac{\sigma^2 \tau_c^2}{\lambda^4}.$$ (4.0.3)

From these equation we can evaluate, that surface roughness is one of the main factors for light scattering appearance on the surface [25]. So surface roughness is a big factor for creating marks with good contrast, especially marking glass and glass-ceramics for achieving good contrast.

5. Nonlinear processes in laser marking using ultrashort pulses.

In our work we are using ultrashort impulses for ceramic ablation. When laser intensity gets high enough nonlinear absorption appears in the material also. In our research 190 fs work pulse even with highest repetition rate reaches 0,4 GW peak intensity and such power is enough to cause nonlinear absorption and plasma formation in the material. These processes increases absorption and lower the transmittance in the material and causes material to vaporize and melt [26, 27].

5.1. Two photon nonlinear absorption.

Two-photon absorption (TPA) is a nonlinear absorption mechanism which causes transition from the ground state of a system charges to jump into higher state energy levels by absorbing two photons. There can be two possible TPA cases shown in Fig. 12, in one case two photons from the same optical field oscillating frequency ω are absorbed to make transition to higher energy levels which is approximately resonant at 2ω. In second situation, two different photons with different optical fields at frequencies ω_e and ω_p is absorbed which approximately resonant at $\omega_e + \omega_p$. First case usually appears and generated by one pump beam and other case can be caused by different probe beam. In both cases the intermediate state is not real and doesn't involve real stationary state of the system [26, 27].
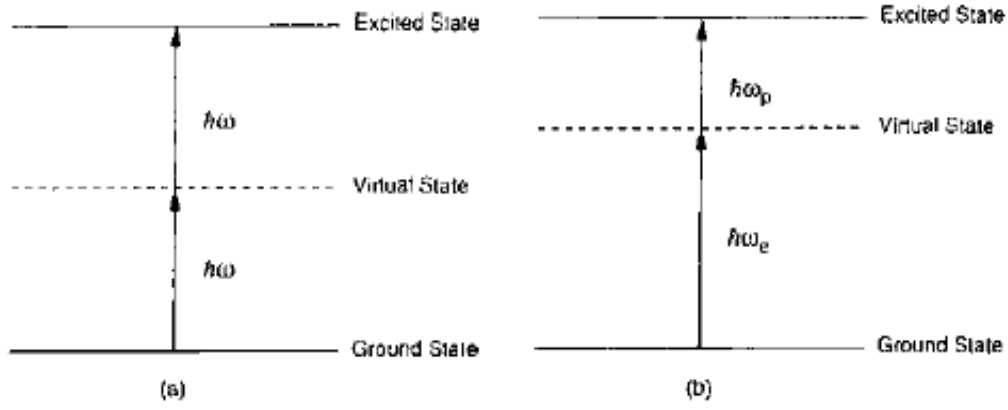
Fig. 12. Schematic of TPA. a) TPA of two same frequency photons and b) TPA of two different frequency photons [26].

The nonlinear absorption is proportional to the scare of entering intensity:

$$\frac{dI}{dz} = \alpha I - \beta I^2, \tag{5.1}$$

where α is the linear absorption coefficient due to the presence of impurities and β is the two-photon absorption coefficient. In the materials imaginary part of $\chi^{(3)}$ (4.1) determines the strength of the nonlinear absorption and β is also determined by two photon absorption cross-section σ_2 (4.2):

$$\sigma_2 = \frac{\hbar\omega\beta}{N_o}. \tag{5.1.1}$$

Where $\hbar\omega$ is photon energy and N_0 is atom or molecule density in the material.

$$\beta = \frac{3\pi}{\varepsilon_0 n^2 c\lambda} Im(\chi^{(3)}), \tag{5.1.2}$$

where ε_0 is relative permittivity, n is refractive index of the material, c is speed of light.

A. Dubietis et. al. in their work analyzed TPA properties in their work, how transmission of the phase-matchable crystal changes due to TPA in three different crystal with different TPA coefficient. By increasing intensity values of transmission decreased and to materials with higher β transmittance value decreases faster (Fig. 13) [28].
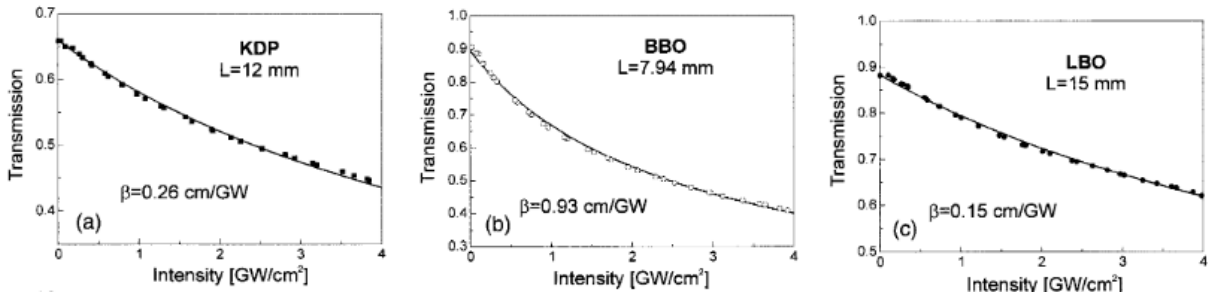

Fig. 13. Intensity-dependent transmission curves for KDP, BBO, LBO crystal samples measured at 264 nm [28].

5.2. Three photon or multiphoton nonlinear absorption.

When intensities get even higher three photon or multi photon absorption can be detected in the materials. In these cases three or more photons gets absorbed in the material. Three photon absorption (3PA) can be described:

17

$$\frac{dI}{dz} = \alpha I - \beta^{(3)} I^3. \tag{5.2.0}$$

Where $\beta^{(3)}$ is three photon absorption coefficient, which is related to to $\chi^{(5)}$ imaginary part:

$$\beta = \frac{5\pi}{\varepsilon_0^2 n^3 c^2 \lambda} Im(\chi^{(5)}). \tag{5.2.1}$$

To achieve higher order photon absorption you need intensity much higher order. It's hard to register or detect and analyze such processes, because more processes appears when intensity increases like plasma formation, ionization, charge avalanche. 3PA can have even more different frequencies and more beams so to predict this absorption is even harder to express in formula (Fig. 14).
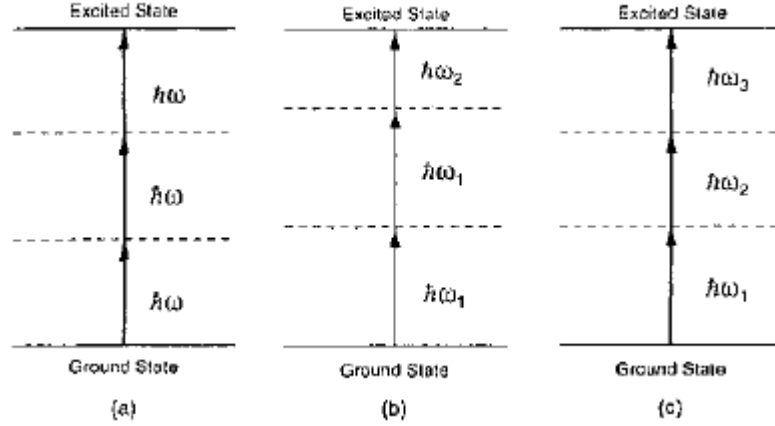

Fig. 14. Schematic diagram of three-photon absorption (3PA). (a) Single beam self-3PA; (b) two-beam 3PA; and (c) three-beam 3PA [26].

The analog formula for multi-photon absorption can be expressed:

$$\frac{dI}{dz} = -\left(\alpha + \beta^{(K)} I^{K-1}\right) I. \tag{5.2.2}$$

5.3. Plasma formation through nonlinear absorption, ionization and linear absorption.

Plasma creates when gas or part of gas is ionized. Plasma can be generated through nonlinear processes – multi-photon absorption, ionization or linear absorption, but plasma and laser beam interaction are nonlinear. Main part of plasma creation is free charge generation. When we affect charges with high intensity beam, we can express free charge generation:

$$\frac{dN^e}{dt} = \frac{dN^i}{dt} = \left(N_o - N^i\right)\sigma_K I^K - a N^e N^i, \tag{5.3}$$

here σ_K- K- photon absorption cross-section, a – electron and ion recombination speed, I – intensity of laser beam. When pulses are ultrashort in that case charges won't recombines to ground level so number of free charges is continuously generated. When this process appears value of relative permittivity of the material changes. Through relative permittivity we can describe plasma frequency (ω_p):

$$\omega_p^2 = \frac{N^e e^2}{\varepsilon_0 m}. \tag{5.3.1}$$

Plasma frequency value changes depending on free electron density N^e value. When plasma frequency value is $\omega_p^2 < \omega^2$, plasma is transparent, then refractive index of the medium $n = \sqrt{\varepsilon}$ is real and light get through the material. When plasma frequency gets bigger $\omega_p^2 > \omega^2$, refractive index become imaginary so the light will be absorbed or reflected and that's how plasma becomes opaque [26, 27].

When the intensity is gets bigger about 10^{18} W/cm^2, electrons get accelerated and mass of the electron changes. This will affect changes in plasma frequency and refractive index values. From this, through changes of plasma frequency and refractive index, we can express critical focusing power formula [26]:

$$P_{cr} = \frac{\pi}{4} n_0 c (\frac{mc^2}{e})^2 (\frac{\omega}{\omega_p})^2. \tag{5.3.2}$$

6. Ceramic materials and their properties.

In this research glass ceramic material was marked. Our ceramic material are used in induction cooktop and are very brittle but also hard material, opaque in visible spectrum. . For ceramic material usually pulsed lasers are used for marking. [10]. Glass-ceramics also known vitrocerams, pyrocerams, sittals are produced by controlled crystallization of certain glasses induced by additives. Glass-ceramic materials have both amorphous glass structure and crystalline like structure. In most glass-ceramics crystallinity varies between 30-70 percent. Glass-ceramics are free from porosity, but in production process bubbles and pores are created appears. These ceramics have an advantage, because they can be mass produced, possible to design their nanostructure with big variety of materials (Silicates, Phosphates, Oxides). There can be a lot of different ways how to develop glass-ceramics: melting, forming, sol-gel, chemical vapor deposition ant others [29-32].

Glass-ceramics (GCs) posses a good combination of many important properties and most of the properties can be controlled through additives, it has high hardness, good crystalline structure, resistance to moisture or gas penetration, good thermal stability, mechanical strength (up to 500MPa), high temperature deformation, excellent electric insulating properties, zero shrinkage, good chemical durability. In A. Berezhnoi book ,,*Glass-Ceramics and Photo-Sitalls*'' softening temperatures ranges from 452 to 900°C, dielectric constant varies from 5.7 to 6.9 at 1 MHz, density ranges 2.4-2.72 g/cm^3 [34].

In this work ceramic material which we are using usually is used for consumer products, so it has low expansion rate and resistant to thermal shock, have high toughness compared to glass, low thermal expansion. Big impact of ceramic properties have additives, so optical properties, biocompatibility, electric and magnetic properties can properly change because of the additives. For consumer products metal oxide glass-ceramics are used which can contain Li$_2$O, Al$_2$O$_3$, SiO$_2$, CaO, MgO, ZnO, BaO, P$_2$O$_5$, Na$_2$O and K$_2$O. Glass-ceramics with oxides additives relies with high toughness, appealing aesthetics and very low thermal expansion coefficient [29-34].

7. Hydrophobicity.

Surface modification these days let us change visual parameters. Creating microstructures on the surface and ablating material can help us change surface spectrum absorptivity and reflectance which is the main aspect in the marking technology. Although surface modifications and textures can help us reach other mechanical properties of the material surface. One of the main property which attracted main attention to materials science and surface modification is material wettability, which in this work is one of the main aspects to focus on. In this work main focus for our material marking was to create high contrast hydrophobic material. Marked areas on glass-ceramic material gets hydrophilic which largely increase contrast and visible color changes when materials gets wet, water and dirt collects on marked surfaces. By creating hydrophobic surfaces it would deflect our named problems and also could give our marks self-cleaning properties.

Main measured parameter which describes material surface wettability is contact angle between water droplet surface and material surface. How water will spread across the surface and contact angle depends on adhesive and cohesive forces between liquid and solid and surface tension of the solid. Surface tension is more usable to describe and predict materials wettability where surface tension for solids have been divided in to "high energy surface" and "low energy surface". Energy tension force usually describes chemical bond and forces in the material which interacts in the surface. Materials which have strong covalent, ionic or metallic chemical bonds tends to have high energy tension, for example metals, glasses, ceramics. Organic materials or other materials where molecules are held together more by physical forces (e. g., Van der Waals and hydrogen bonds) tends to have low energy tension. Through surface tension contact angle value can be approximated by Young's equation:

$$\cos\theta = \frac{\gamma_{sg} - \gamma_{sl}}{\gamma_{lg}}. \tag{7.1}$$

Where γ_{sg}, γ_{sl}, γ_{lg} is interfacial free energy per unit area of the solid-gas (*sg*), solid-liquid (*sl*) and liquid-gas (*lg*) (Fig. 15) [35].
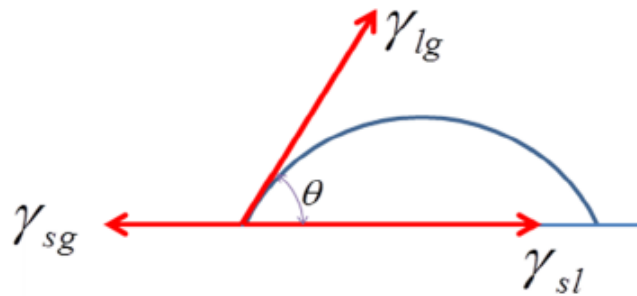

Fig 15. Example of hydrophylic surface and interfacial energy interactions.[35]

If material have contact angle less than 90⁰, material is hydrophobic. When material have contact angle with water more than 90⁰ - material hydrophilic. For superhydrophobic surfaces contact angle with water has to be more 150⁰. When contact angle is less 5⁰, then surface is superhydrophilic. Hydrophobicity strongly describes roll of angle which is closely related to contact angle, but some hydrophobic surfaces has high roll of angle so this value doesn't fully describe hydrophobicity of the surface as there are two types of surface wetting. Surface wetting can be homogenous, when water droplet only connects with solid surface and

heterogenous, when water droplet connects with air and solid (Fig. 16). Homogenous wetting also can be described as Wenzel state of wetting and Heterogenous wetting – Cassie-Baxter state [35-37].
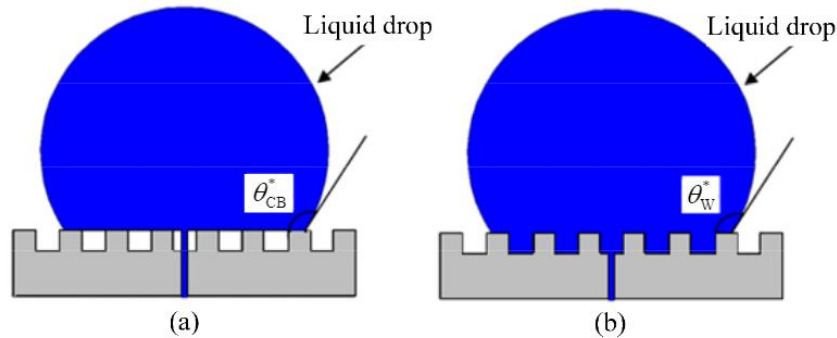

Fig 16. Liquid wetting types. a) heterogenous wetting. (Cassie-Baxter); b) homogenous wetting. (Wenzel) [36]

Homogenous wetting was described by Wenzel, where he states that material surface roughness (r) should enhance material wetting properties according if material is hydrophobic or hydrophilic. Wenzel equation shows how roughness value can change contact angle:

$$\cos \theta_W = r \cos \theta. \qquad (7.1.1)$$

Where θ_W is angle which changes depending on surface roughness. Homogenous wetting can only enhance hydrophilic properties if surface is hydrophilic and hydrophobic properties if surface is hydrophobic, because Wenzel state relies on surface roughness and it's expressed:

$$r = \frac{Real\ surface\ area}{Projected\ surface\ are}. \qquad (7.1.2)$$

So surface roughness value is always more than 1, by increasing surface roughness you only increasing r value. It means from Wenzel state you can not create hydrophobic surface from hydrophilic surface. Wenzel equation can only describe homogenous wetting and if surface wetting is not homogenous, Wenzel equation is not sufficient and more complex model is required to describe and measure contact angle when water interact with various materials on surface [35].

Heterogenous wetting is explained using the Cassie-Baxter model. At heterogenous wetting air gaps are between pillar and water only rest on solid rough surface. In most literature Cassie-Baxter equation is expressed:

$$\cos \theta_W = f_1(\cos \theta_{1Y} + 1) - 1. \qquad (7.1.3)$$

Where f_1 is the fraction of liquid droplet and solid top area. Cassie-Braxter model gets dominant when surface roughness is increasing. So if you decrease surface area on which water is siting and water droplet mostly interact with air, f_1 value can decrease up to 0. When f_1 is decreasing up to 0, $\cos\theta_{1Y}$ value comes up to -1 and from equation θ_W angle approaches 180⁰.

The theory of determination of wetting regime and liquid penetration into roughness was analyzed by A. Marmur in his work where in conclusions he stated that wetting regime can be determined through four steps, which relies on Gibbs energy, surface roughness and fraction. In practical appearance both models have an impact and coexist, but to reach excellent hydrophobicity Cassie-Baxter mode is more important. Cassie-Baxter wetting state reduces

contact area between water and solid surface and can repel water, can have very low roll of angles. This make surface self-cleaning because water droplets will roll off of the surface and when it rolls water picks dust and dirt along the way [35-38].

8. Hydrophobic surfaces.

Superhydrophobic surfaces firstly was discovered in nature. Examples, designs adaption and derivation taken from nature is called "biometric". There are many superhydrophobic examples in animals and plants. One of the main hydrophobic surface example is lotus leaf. Lotus leaf have papillae size at scale of 10-50 µm and distance between them (Fig 17). Most of lotus leaf papillae are covered by nanostructures which size approximately 100 nm. The height of bumps is only about 15 µm and all surface is covered with hydrophobic wax. This structure let lotus leaf contact angle with water to be about 150⁰ [39-41].
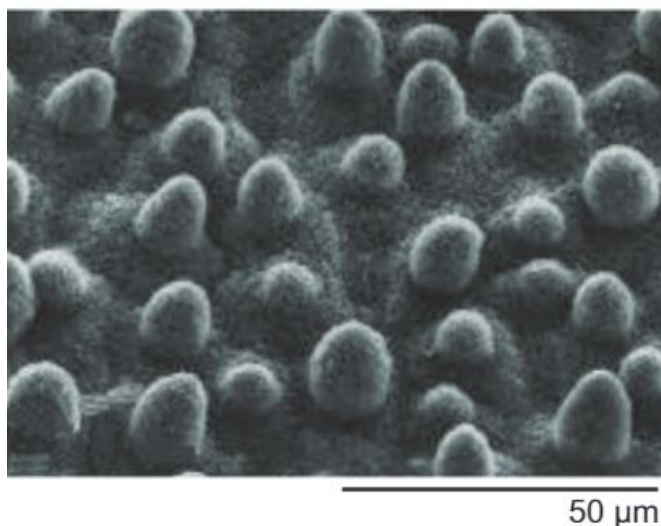

50 µm

Fig. 17. Lotus leaf surface. [40]

Other examples of biometric surfaces and materials which we can detect in nature: butterfly wing, rice leaf, water strider leg, moth eye, shark scales. Many plants have similar surfaces like lotus leaf, but animal biometric examples are more complicated and harder to copy.

To attempt, obtain and make hydrophobic surface mostly is followed by two main principles: to generate micro, nano, micro/nano scale hierarchical surface structures and coat them with low surface energy materials or directly create structures on the low-surface energy materials. The main key for manufacturing these surfaces is the fabrication of the structures which helps to reach hydrophobicity. There are various techniques for fabricating hydrophobic or superhydrophobic surfaces and structures: photolithography, physical/chemical deposition, chemical synthesis, chemical etching, sol-gel methods, template method and laser processing [42, 43].

8.1. Laser textured superhydrophobic surfaces.

Laser processing has a lot of advantages for creating hydrophobic surfaces. It is non-contact, maskless, programmable, one-step fabrication. This processing type is not only promising for scientific purposes, but also have huge potential for realistic practical applications. The surface structures made by laser processing can be divided into two main types: arrayed microscale structures and laser-induced structures which are random or periodic nanoscale structures. To create microscale and nanoscale structures mostly ultrashort pulses are used, because it can generate ultrahigh beam intensities, smaller areas are affected on the surface and it is usable on various solids without significant material dependency. Laser processing is unique technique, because you can change and adapt required laser parameters. It can have big impact on structures and lets to control structure size, shape, roughness depending on laser wavelength, pulse duration, pulse repetition rate, pulse energy, focused beam size, scanning speed [42, 43].

8.1.1. Laser processed hydrophobic surface examples on various materials.

In this work we took five laser processing examples to create hydrophobic surfaces which were created on glass materials. On first three research paper hydrophobic surfaces were created by fabricating periodic microgratings on sample surface on soda lime glass, solar glass and silica glass. In other works hydrophobic surfaces were created by making rectangular pillars on the glass or point by point pattern. In all researched articles samples after laser ablation were coated with hydrophobic material, mostly with fluoroalkysilane (tridecafluoro-1,1,2,2-tetra-hydroctyltrichlorosilane ($CF_3(CF_2)_5(CH_2)_2SiCl_2$) [44-48].

Sh. Ashan and others used Ti:sapphire femtosecond laser with central wavelength of 786nm with a repetition rate of 1 Khz, pulse width 183 fs. They created microgratings, where scanning step was 10 µm and pulse energy was 21 µJ, scanning speed 5 mm/s with two iterations (Fig 16). In the final result they got hydrophobic surface with contact angle of 155⁰ [44].

L. Boinovich, A. Domantovskiy were creating similar microgratings with second harmonic wavelength of 515 nm, changing repetition rate between 50 kHz and 500 kHz, pulse energy 4 mJ, pulse width 200 fs, focused beam diameter 7 µm ($1/e^2$ level), scanning speed up to 6 mm/s. They created hydrophobic surface with contact angle ranging from 156,8⁰ up to 166,6⁰ (Fig. 18) [45].
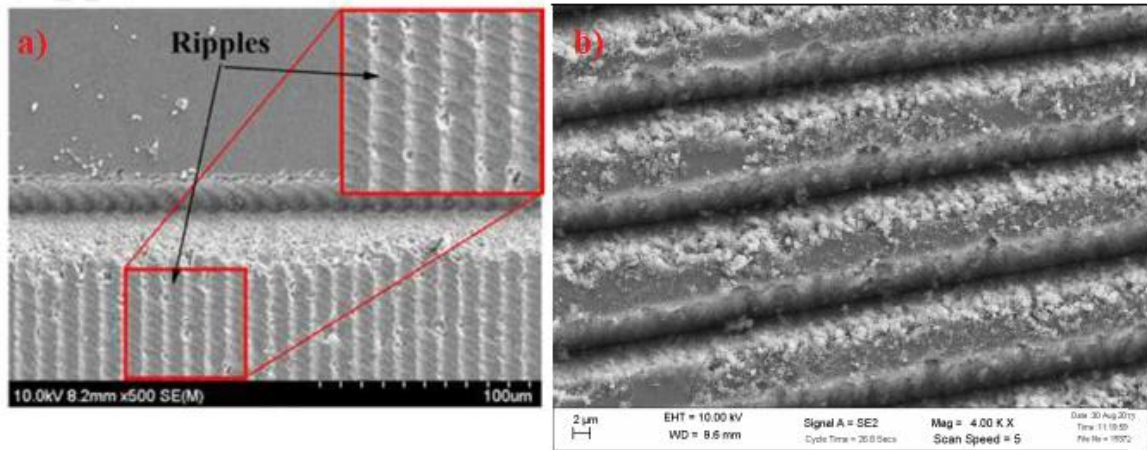
Fig 18. SEM image of the periodic gratings. a) created in Sh. Asham work; b) created in L. Boinovich work [44, 45].

B. Wang, Y. Hua and other were creating groove-shaped arrays on solar glass. They used Nd:YVO$_4$ laser system with central wavelength of 1064 nm, pulse width 10 ps, repetition rate of 400 kHz, pulse energy 35 µJ, scanning speed 300 mm/s . They created several examples with different scanning step: 50 µm, 55 µm, 60 µm, 65 µm, 70 µm, 75 µm. In their work results tendency was noticed, that by increasing laser line interval – contact angle value decreases (Fig. 19) [46].
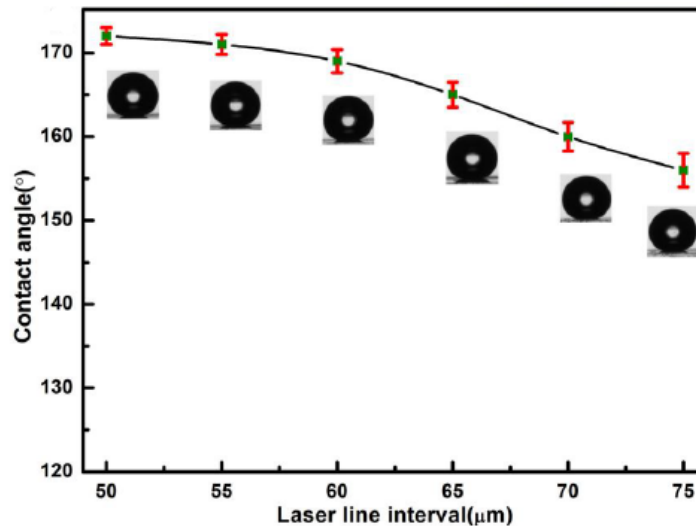

Fig 19. Contact angle dependency from laser line interval [46].

Other method to create hydrophobic surface is point by point ablation in glasses. This method used Y. Lin with his team and it lets to have bigger spot of focused beam which was 35 µm. By variating iteration times (from 2 to 5 times), pulse energy (from 20 µJ to 100 µJ) and distances between pulses (20 µm and 30 µm) they were able to get contact angle from 140⁰ up to 165⁰. The sliding angle was low in their hydrophilic samples about 1-2⁰. Also laser treated glass was remained transparent (90% transparency in spectrum range from 300 nm up to 1000 nm) [47].

H. Nguyen with other were creating rectangular shaped pillars by variating their size, distance between them and iteration time (Fig. 20) [48].
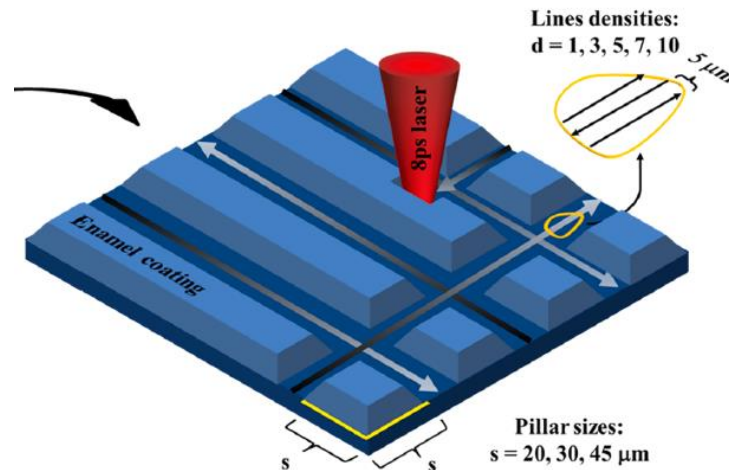

Fig 20. Schematic figure of preparing laser textured hydrophobic surface in H.Nguyen work [48].

When changing line density pillar size, height and depth in report was increasing. Iteration number had most impact on pillar height. Pillar height in most samples with one iteration were about 20 µm, but with four iterations pillar size increased up to 40 µm. Fig. 19 shows that samples with high iteration number already had almost perfect superhydrophobicity not depending on line density that much where other examples was more dependant on line density (Fig. 21). Using this method perfect superhydrophobic surfaces were created with contact angle near 180⁰ and roll off angle lower than 10⁰ [48].
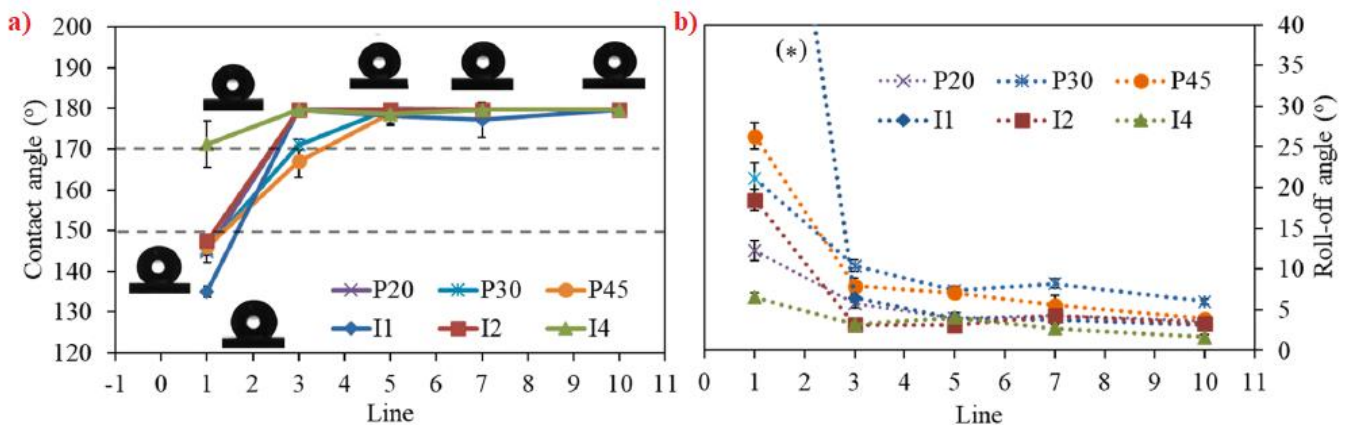

Fig 21. a) Contact angle and b) roll-off angle of silanized laser-textured enamel coating relation on line density [45].

With presented laser texturing methods there are other material examples, when hydrophobic surface was created. On oxide ceramics surface with contact angle about 160⁰ was made texturing rectangular shaped texture with the size of 10 µm and distance of 5 µm [49]. On platinum hydrophobic surface was made creating microgrooves with groove spacing of 100 µm and depth 75 µm. Water contact angle on surface was measured to be 158⁰ and roll off angle only 4⁰ [50].

9. Laser marking equipment for experimentation and marking parameters.

In this work I used two different laser marking systems with two different lasers (Fig 22). Laser beam was directed to laser scanning system with reflective mirrors. First marking system contained Carbide (model CB5-SP) laser from Light conversion. CB5-SP Carbide laser generates maximum power of 5 W, shortest pulse duration 190 fs, maximum pulse energy > 100 µJ, repetition rate can vary 60 kHz – 1000 kHz, pulse duration adjustment range from 190 fs to 10 ps and generates 1030 nm center wavelength (error can be about 10 nm) [51]. In first marking system galvo scanner IntelliSCAN 14 from SCANLAB was used, which can work in 450-2500 nm wavelength range, with marking speed of 2 m/s and image field size 95 mm. x 95 mm. Galvo scanner was mounted with f theta lens with focus length of 100 mm. Also motorized high-load vertical positioning stage from Thorlabs MLJ150/M with theoretical 1 nm. resolution for finding focus position. Before working with first system you have to be sure that laser beam is perfectly adjusted with scanning system and focus point position is fixed on the surface of the sample. In this system marking patterns and Z axis positioning and laser parameters can be controlled through computer. Focus position in this system have to be found manually by changing Z axis position when marking and looking through microscope in which position marking width is most narrow.

Second marking system is more automated and it contains two different galvo scanners (Fig. 22). In second Carbide (model CB3-40W) laser was used. CB3-40W Carbide laser generates maximum power of 40 W, shortest pulse duration 290 fs, maximum pulse energy > 0.8 mJ, repetition rate can vary 100 – 2000kHz, pulse duration adjustment ranges from 290 fs to 10 ps and generates 1030 nm center wavelength (error can be about 10 nm).[19] In second system laser can generate more average power and higher energy pulses than CB5-SP laser. In this system for marking with first harmonic wavelength faster scanner was used excelliSCAN14 from SCANLAB with working wavelength range 350 nm – 1064 nm, image field size 95mm x 95mm and higher marking speed 4 m/s and mounted with f theta lens with focal length of 100 mm. and working range 1030 – 1080 nm. Second scanner is used for marking with third harmonic wavelength in UV range and is similar to the first system scanner and it's mounted with f theta lens (λ – 355 nm, f = 100 mm). Second system also contains XY positioning table 8MTL220 from STANDA for moving the sample between the scanner and camera. Everything in this system is automated with DMC software. With the help of the camera we can see surface of the sample and adjust focus position through software analyze and see results instantly. With DMC software it was easier to program cutting patterns and marking parameters (focus position, cutting angle rotation, controlling laser power, marking speed, pulse picker) because it is connected to laser. In both systems beam was directed using reflective optics, so laser beam power on the surface of the samples is lower than laser beams power just lighted from the laser.
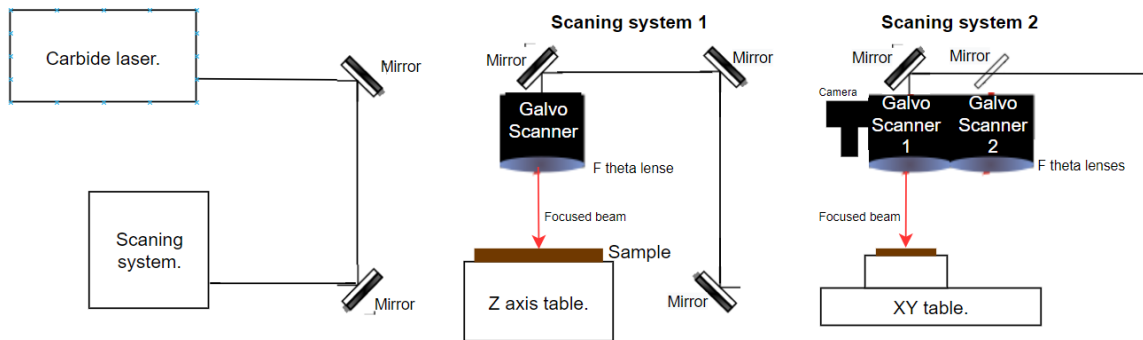
Fig. 22. Schemes of two marking systems. In Scanning system 2 two galvo scanners are used – one for marking with first harmonic wavelength and second with third harmonic wavelength.

First marking system focused beam size was about 20 µm, when laser wavelength was 1030 nm and 15 µm working with second harmonic. Surface pictures were taken and analyzed using Olympus Bx51 microscope. Surface profile was analyzed with Sensofar plµ 2300 profilometer.

9.1. Marking parameters for finding good contrast.

In first marking system I made research how marking contrast changes when we change pulse repetition rate, pulse duration, distance between marking spots and repeat number of the same marking. We were marking 5mm x 5mm rectangular shape marking, when we were doing marking couple times of the same spot, each time marking line deposition was changed by 90⁰ Average laser power of the system – 3.9 W. From power value we can see, that reflective optics decreases due losses and absorption decreased the power. Marking parameters were:

- Repetition rates were: 60.1 kHz; 100 kHz, 250.7 kHz, 603 kHz.
- Pulse duration: 243 fs, 1 ps, 2 ps.
- Programmed distance between marking spots: 2.5 µm, 5 µm, 10 µm, 15 µm, 20 µm, 30 µm, 50 µm, 100 µm.
- Repeat times:1, 4 and 8 times.
- Wavelength: 1030 nm.

Sometimes we had to adjust pulse picker (PP) parameter to get bigger distances between marking spots in the mark, because marking speed of the scanner was too slow. PP parameters were changed at higher frequencies.

In second marking system I made research how marking contrast changes when we change laser power, pulse duration, distance between marking spots and repeat number and Burst-in-burst (Biburst) values. Only repetition rate of pulses remained the same – 100 kHz. We were marking 3mm x 3mm rectangular shape markings, when we were doing marking couple times of the same spot, each time marking line angle was changed by 26⁰. We used 26⁰ angle because when increasing marking times on the same spot pulses won't get shot in the same position.

Marking parameters were:
- Laser power: 1%; 5%, 10%, 20%, 35%, 50%, 100%.
- Pulse duration: 243 fs, 1 ps, 2.5 ps, 5 ps, 10 ps.
- Programmed distance between marking spots: 5 µm, 10 µm, 15 µm, 20 µm, 30 µm, 50 µm, 100 µm.
- Repeat times: depended on laser power and distance between marking spots.
- Biburst options: p=2 and n=1; p=4 and n=1; p=4 and n=2; p=1 and n=4; p=2 and n=4;
- Wavelength: 1030nm.

For Biburst option change I only used 243 fs pulses. Also with second marking system marking with third harmonic wavelength was made. Laser power was 7.86 W, repetition rate: 602.7 kHz, but we didn't get satisfying results.

9.1.1. Burst with burst laser mode

Biburst laser mode is tunable laser modes which generates GHz and MHz bursts. The difference between standard and biburst mode is that standard mode releases pulses at some fixed frequency but Biburst mode emits laser pulses in packets instead of single pulses. Biburst mode gives an advantage for ablation processes. For better heat accumulation in standard mode you need to increase laser pulse repetition rate but Biburst mode lets to get same or better results in lower repetition rates. Subsequent pulses in Biburst mode can preheat the sample and duo to heat accumulation required energy to evaporate the material can be lower. Working with higher repetition rate excess thermal energy can be generated as GHz burst laser mode is able to remove excessive thermal energy with successive pulses [52].

Fig. 23 shows visual explanation of Biburst mode. Carbide lasers lets you adjust aplitude slope, which can have and impact on heat accumulation rate and adjust number of pulses in the MHz and GHz burst packets. For Carbide-CB3 model GHz-Burst can have up to 10 pulses in it and intra burst period is about 440 ps, MHz-Burst can also have up to 10 pulses in the burst packet and intra burst period is about 15 ns [51].
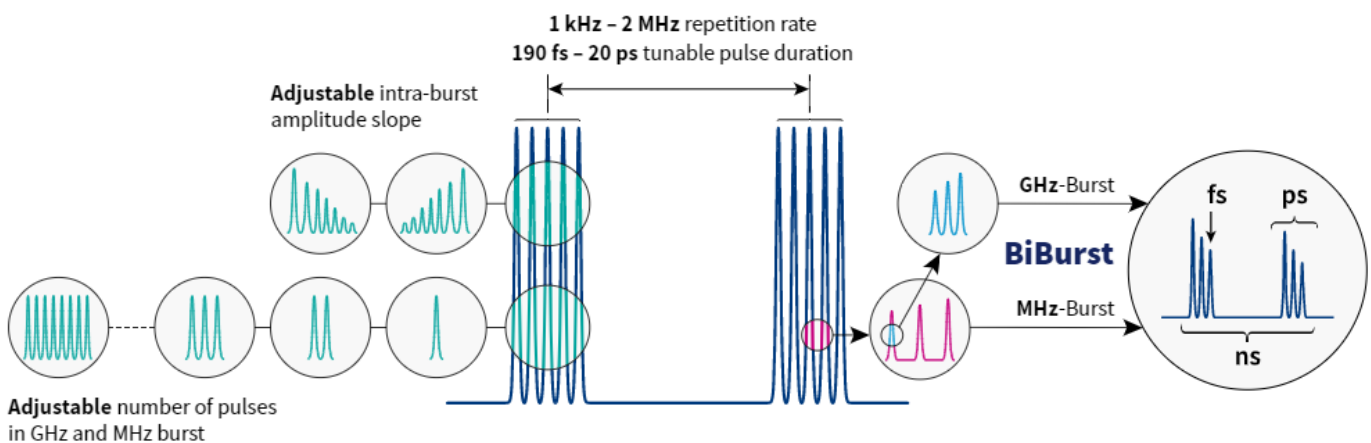

Fig. 23. Visual explanation of Biburst mode [51].

9.2. Marking parameters for hydrophobic surface creation.

Only first marking system was used to create hydrophobic surfaces. First and second harmonic were used. Laser power of the first harmonic was 3,6 W, second harmonic:1.44 W. Three layouts were used for creating hydrophobic surfaces: microgratings, squared pillars and point by point ablation. Point by point structure was used for finding good contrast so marking parameters are mentioned before. For creating microgratings for one iteration laser beam was scanned two times, one time laser scans in one direction on the second scanned on the opposite direction. Marking parameters were:

- Repetition rate: 60.1 kHz; 100 kHz, 250.7 kHz.
- Pulse duration: 243 fs, 1 ps, 2 ps.
- Programed distance between lines: 5 µm, 10 µm, 15 µm, 20 µm, 30 µm, 40 µm, 50 µm, 80 µm.
- Iteration times:1, 2, 4, 8, 12, 20, 32, 50, 100.
- Scanning speed: 100 mm/s, 150 mm/s, 200 mm/s, 300 mm/s,

For creating squared like pillars laser beam was programed to draw lines in certain periodic lines, line deposition angle was changed by 90º four times so laser beam was scanned two times on horizontal and vertical axis. Changeable marking parameters were:

- Repetition rate: 60.1 kHz; 100 kHz, 250.7 kHz.
- Pulse duration: 243 fs, 1 ps, 2 ps.
- Programed distance between lines: 10 µm, 20 µm, 30 µm, 35 µm, 40 µm, 45 µm, 50 µm, 80 µm.
- Iteration times:1, 2, 4, 8, 12, 20, 50.
- Scanning speed: 100 mm/s, 150 mm/s, 200 mm/s, 300 mm/s.

After laser texturing we also immersed our glass-ceramic material into solution for 24 hours to create hydrophobic film on the surface. Solution was made of 0.11% hexamethyldisilazane $((CH_3)_3SiNHSi(CH_3)_3)$ and 0.89% toluene $(C_6H_5CH_3)$. After immersing we dried our sample in the oven for an hour.

10. RGB value measurement.

In this paperwork we were measuring Red-Green-Blue (RGB) values for marked spots. Our ceramic material is dark brown color and main focus of this work to get white marks on the material. RGB values were measured using phone HUAWEI Mate 10 pro CMOS camera and ,,Adobe Photoshop 2020'' application. Measuring scheme is shown in Fig. 24, in measurement scheme there were two light sources, one of them LED lamp, 2700 K, 1521 lm, other halogen table lamp, which specification I could not find. In this measurement we manually calibrated white color using white paper. So through all sample plot white papers RGB values would be (250, 250, 250) [53].
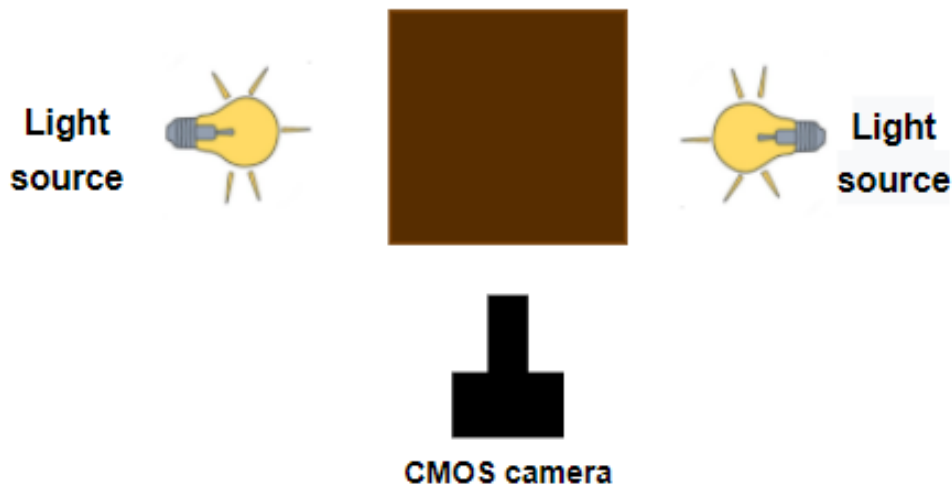
Fig. 24. RGB measurement scheme. It contains two lamp sources and CMOS camera.

It is noticeable that this measurement would have some errors, because lamp emits warm white color, so red color values will be higher when it won't reach maximum values of RGB even when camera was calibrated, this could be caused because of two different type of lamps. Calibration of white color was more difficult with phone camera, because it's not professional camera, so we couldn't reach required parameters for white color calibration. For example, suggesting light source phone had only it own programmed choices so you couldn't make white color balance. That why in results RED values always was higher. Also it is mentionable that true RGB values of white paper are not R:250; G:250, B: 250 it can have error about 10 points, depending on the paper [54].

11. Measurement of light scattering.

Measurement of light scattering on our sample was made using experimental setup presented in Fig. 25. This setup is used for total integrated scattering to measure surface roughness. In this work we didn't use computer for roughness calculation instead we compared how much second harmonic wavelength (532 nm) scatters from our samples in comparison of ideal scattering example which scatters over 99 % of the light. This measurement is based on collection of scattered light with integrated Ulbricht sphere which helps to collect scattered light in wide angular range (from 2º to 85º) and directs to the detector and it's usually used in visible and IR regions. In this experimental setup Nd:YAG Q-switched laser (Ekspla NL 202) is used which operates at 1 KHz repetition rate, wavelength of 1064 nm and able to generate second harmonic (532 nm) and third harmonic (355 nm) wavelengths. Half-wavelength plate and thin-film polarizer is used for pulse energy attenuation. Two apertures allows to get homogenous beam into the sample with M^2 better than 1.3. Beam diameter, which are directed to the sample, is about 0.4 mm.
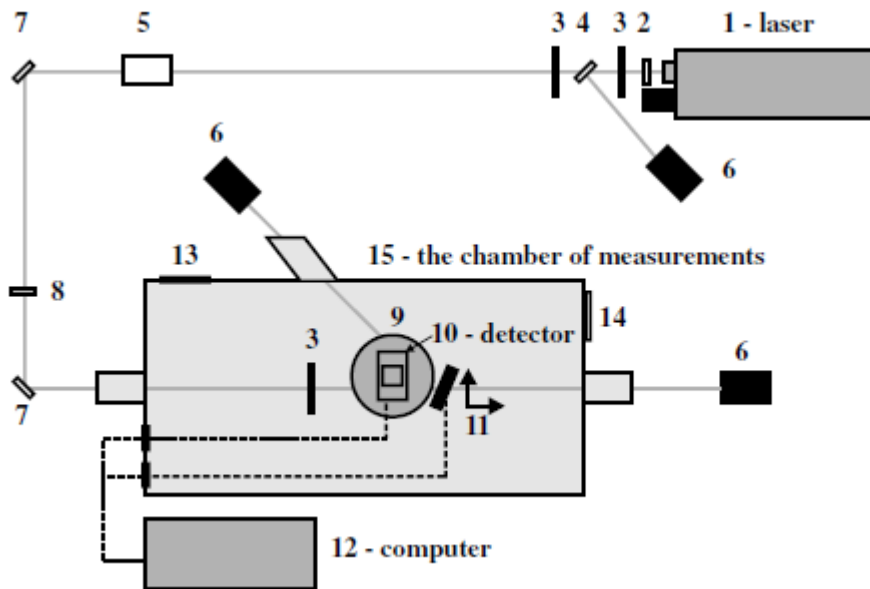
Fig. 25. TLS measurement setup (1 - laser with harmonic generators, 2 -half-wavelength plate, 3 - aperture, 4 - thin-film polarizer,5 - attenuator based on neutral filters, 6 -beam dump, 7 -mirror, 8 – 1 m focal lens, 9 - Ulbricht sphere, 10 -detector, 11 -translation stage, 12 - computer, 13 - clean air flow, 14 - return air flow, 15 - the chamber of measurements).

12. Results and analysis.

In this research over 2800 samples were made. In the first part of research 2500 samples were made to find good contrast values. 300 samples were made trying to create hydrophobic surfaces. For contrast finding I worked with second marking system mostly which is more advanced and it's easier to manufacture and program new samples, scanning speed was bigger and templates were simple. To get good contrast on our glass ceramic material main point was to create white mark with RGB values near 250, our glass ceramic material has RGB values of (20:20:20).

For surface wetting study we only worked with first marking system which is slower to operate. Due to the global pandemic and restrictions it was harder to get to the laboratory and do the practical task, which led to some mistakes and time shortage. Time shortage didn't let to do more samples, variate between marking parameters more and analyze more deeply our created structures.

12.1. Marking contrast dependence on laser power, pulse duration and Biburst mode.

Laser power for contrast changes doesn't have big influence when we worked with 243 fs pulses in standard mode, because laser pulse interaction time with the material was not high enough to accumulate heat in the material and make large visible changes (Fig. 26). In our case longer pulses creates larger heat affected zone and make bigger contrast changes, but even with increasing laser power it reaches it's limit to create bigger contrast and white marks. 10W it's enough to create marks with RGB values about 200:200:200 when pulse duration is 10 ps.
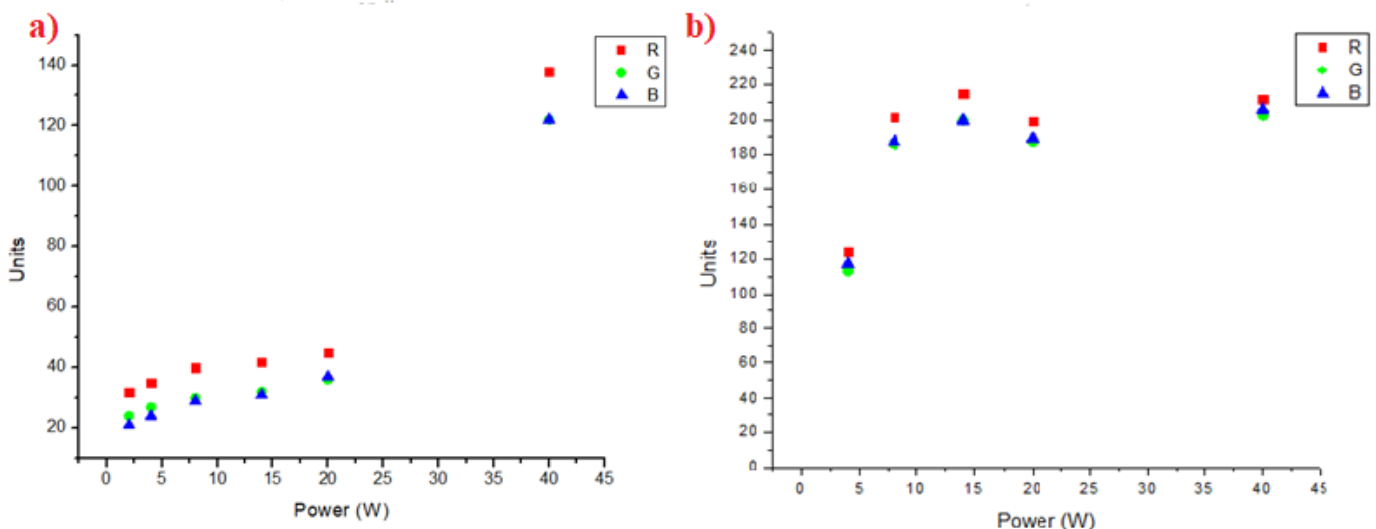

Figure 26. RGB value dependance on power. Marking distance between mark spots is 5µm, at repetition rate 100 kHz, marked one time. a) pulse duration 243 fs, b) pulse duration 10 ps.

This means that increasing power to higher rate is not beneficial for us and in standard laser working regime most of the energy get wasted if we focus on getting good contrast and it can only create unnecessary damage to our markings when pulse duration is 243 fs, microcracks appears on mark and some of the parts drop of the material (Fig. 27).

Fig. 27. Poor quality marking example made by femtosecond pulses. Marking layer peels and can easily be scratched off.

Best changes depending on laser power were noticed when we work with 243 fs impulses using BiBurst mode because it helps to accumulate more heat in the material (Fig. 28). Femtosecond pulses doesn't create deep marks as picosecond pulses. For example white mark, marked with femtosecond pulses using Biburst mode and had higher energy (200 µJ), was 50 µm deep while marks marked with 5 ps pulses was 220 µm deep with pulse energy of 140 µJ.
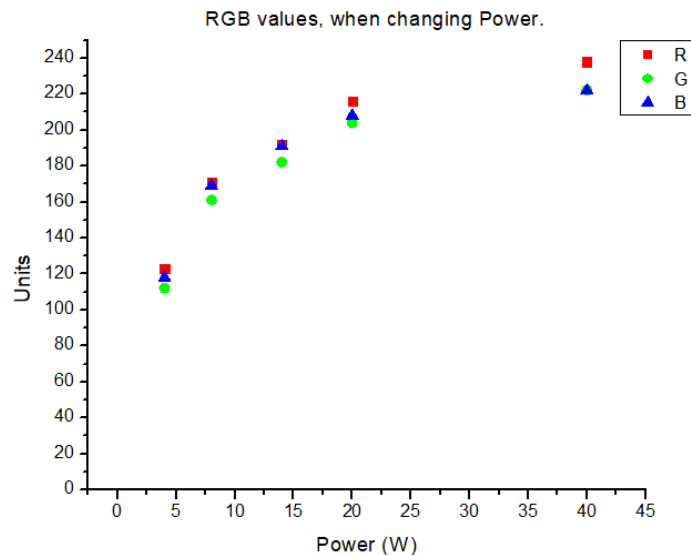

Fig. 28. RGB value dependance on power. Marks created with 211 ps pulses using Biburst mode (p=4, n=2), 100 kHz repetition rate, distance between mark spots is 5 µm, marked one time.

Laser pulse width has big impact for creating better marking contrast on glass ceramics. Marking areas where we marked material with longer pulses created better contrast and in 2,5 – 10 ps we got good results good marking contrast and white color generation. In the result (Fig. 29) it is noticeable that 2,5 ps. and longer pulses could be able to generate white color marks even when laser power, pulse repetition rate and other parameters don't change. By using Biburst mode perfect white color samples can be generated with femtosecond pulses. The main disadvantage of longer pulses, that affected area of the material that laser affected area it's larger and we cannot work with them to create precise textures on material surface which is very important factor creating hydrophobic surfaces. Nonetheless longer pulses can be beneficial to create good contrast on the top of textured microarrays as in this work we got good contrast working with the first system with lower pulse energies (14 µJ).
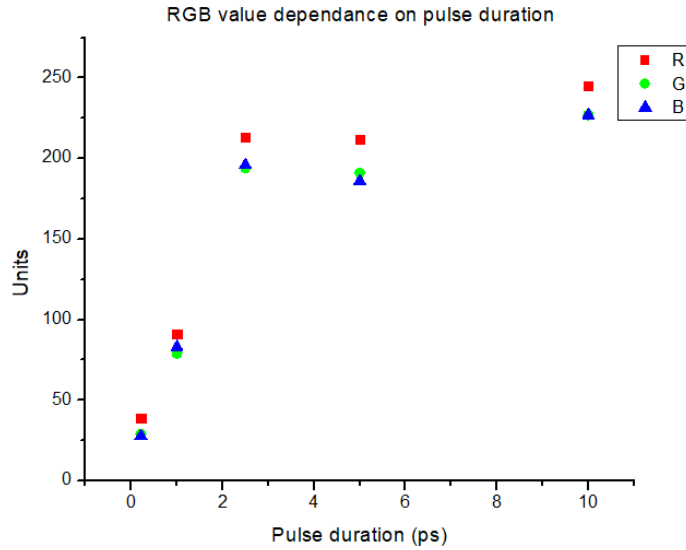
Fig. 29. RGB value dependance on pulse duration (211 fs – 10 ps.). 100 kHz repetition rate, distance between mark spots is 5µm, marked one time, pulse energy 140 µJ. No Biburst mode.

12.2. Marking contrast dependence on iteration, space between marking points, scanning speed.

Iterations doesn't make huge difference while creating good contrast, and in most examples RGB values only improves a little (Table 3) and its clearly visible on Fig. 30. It is irrelevant to increase iterations for contrast gain because it doesn't create good contrast or increase RGB values how we need and only deepens the mark, especially working with picosecond pulses.

| Space between marking spots, µm | Times of repeat | Laser Power, W) | Biburst mode | | R | G | B |
			p	n			
20	2	20	2	4	62	56	58
20	16	20	2	4	46	41	42
20	1	40	2	4	73	74	76
20	4	40	2	4	50	47	54
15	1	14	1	4	96	89	96
15	18	14	1	4	78	77	85
20	1	20	1	4	123	113	121
20	16	20	1	4	79	77	90

Table 3. Example, when mark gets darker duo to increase of repeat times. Pulse width:243 fs; pulse repetition rate: 100 kHz.
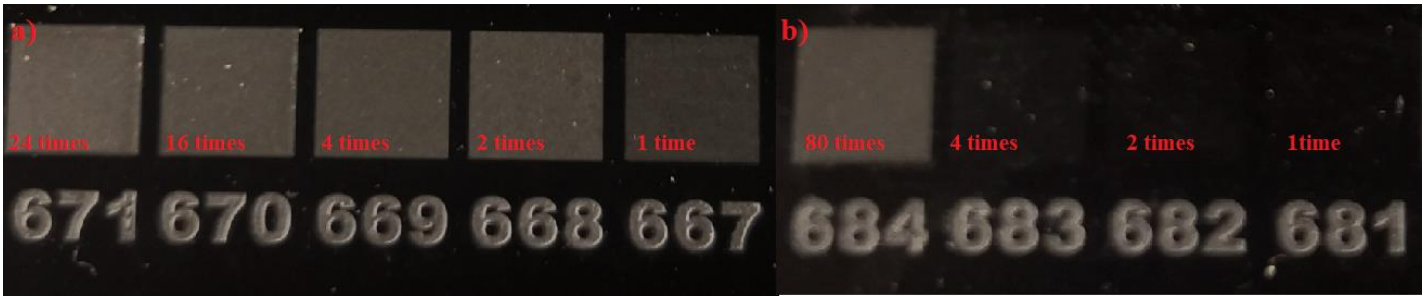
Fig. 30. Contrast changes by increasing marking repeat times. a) Example, how color don't change significantly (repeat time increases from 667 to 671), distance between marking spots 20 µm. b) Color change duo to increasing repeat time (repeat time increases from 681 to 684), distance between marking spots 20 µm.

A big dependance on the marking contrast can be seen when we change the space between marking spots while changing space between marking spots from 5 µm to 100 µm. (Fig. 31) When laser pulse was shot in interval of 5 µm a big RGB value increase was noticed and main reason of that was pulse overlapping. As we know our focus size is approximately 20 µm which means that pulses overlap between each other is about 75%.
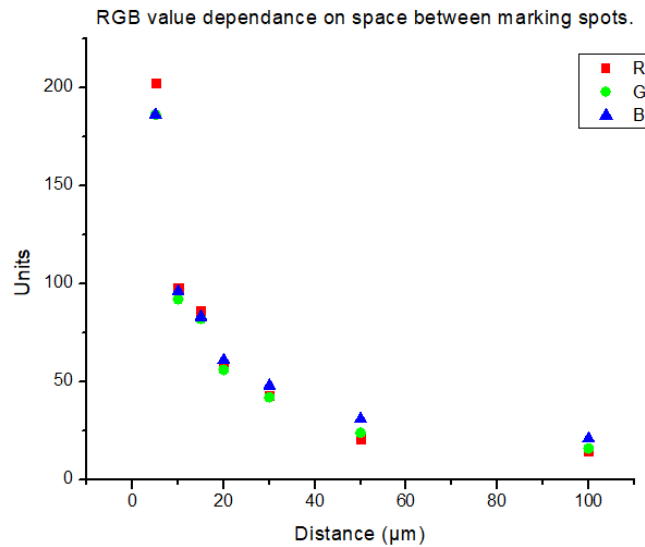

Figure 31. RGB value dependance on distance between marking spots. 100 kHz repetition rate, marked one time, pulse energy 200 µJ. No Biburst mode.

With such high pulse overlap mark surface are very plain reaching rms height of only couple micrometers (Fig. 32). Two samples which had good RGB values were looked under profilometer. One sample was marked using picosecond pulses and other one using femtosecond pulses. Sample marked with femtosecond pulses has roughness of 2.6 µm and sample marked with picosecond pulse had roughness of 8 µm.
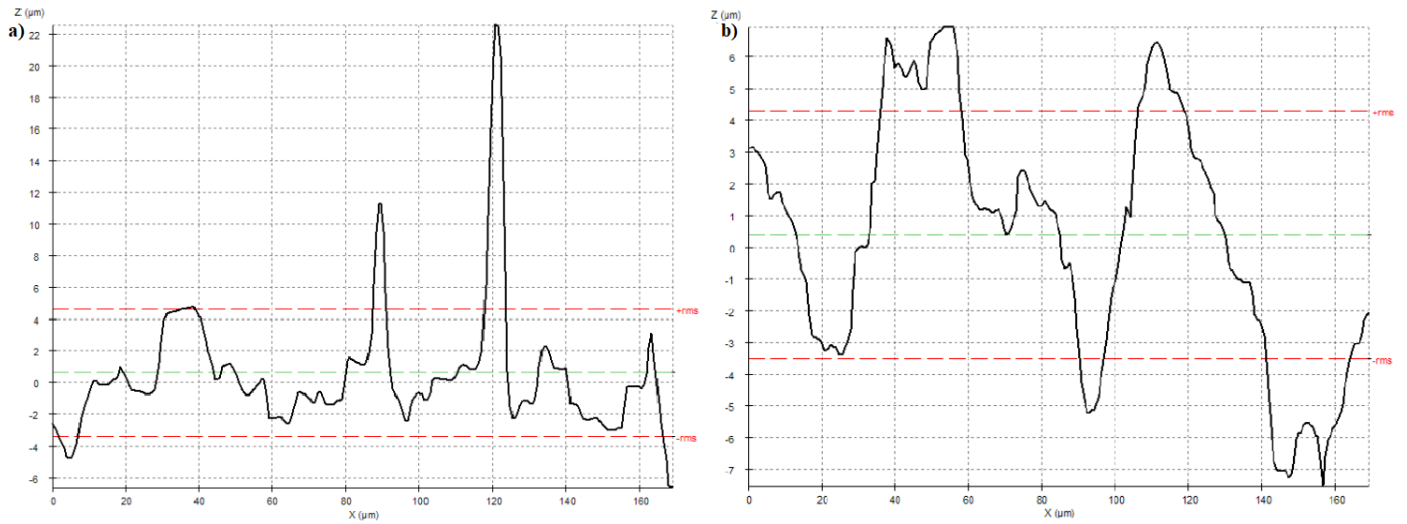
Fig. 32. Surface profile image of mark marked with a) femtosecond pulse (Biburst mode, pulse energy 200 µJ; b) picosecond pulses (pulse energy 140µJ)

Furthermore, by increasing pulse overlapping, I was able to create more white marks even with lower pulse energy 14 µJ and 36 µJ. Pulse overlap was controlled changing scanning speed and pulse repetition rate marked area had also very plain surface with 5.86 µm roughness (Fig. 33) and mark depth was 40 µm. Even though pulse energy was lower mark depth value is too high if we want to create good contrast on hydrophilic surfaces. To decrease mark depth we should find good parameters working with femtosecond pulses using Biburst laser mode, but second laser mark system was not accessible on that time.
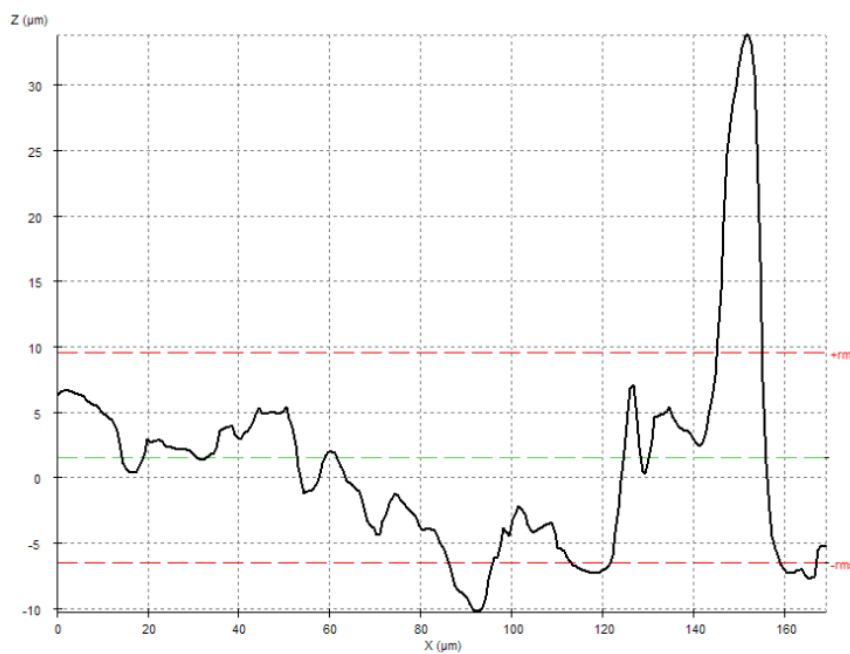

Fig. 33. Surface profile image of mark with high pulse overlap. Pulse duration: 1 ps; Scanning speed: 200mm/s, pulse repetition rate: 251 kHz, pulse energy 14 µJ.

12.3. Light scattering results.

In this measure we compared how much our sample surface scatters light compared to the ideal scattering surface, which have reflection of the light about 99%. We took light scattered results and made proportion to the ideal sample. If our sample would scatter light perfectly as our ideal sample proportion value would be 1. For polished but untreated glass-ceramic surface proportion value with ideal sample was 0.0001. As the results show maximal proportion value of checked marks was ~0.4, this means that surface roughness modification and enhancing light scattering is one of the main factors in creating good contrast on our usable glass-ceramic material. None of our samples had so big light scattering effect as ideal sample, and it could be also related to the strong light absorption of the used glass-ceramic in the visible range and reduction of the scattered light part due to multiple reflections. As could be seen from Fig. 34 the laser power doesn't have much an impact on scattering results when sample was marked using longer pulses (5 ps).
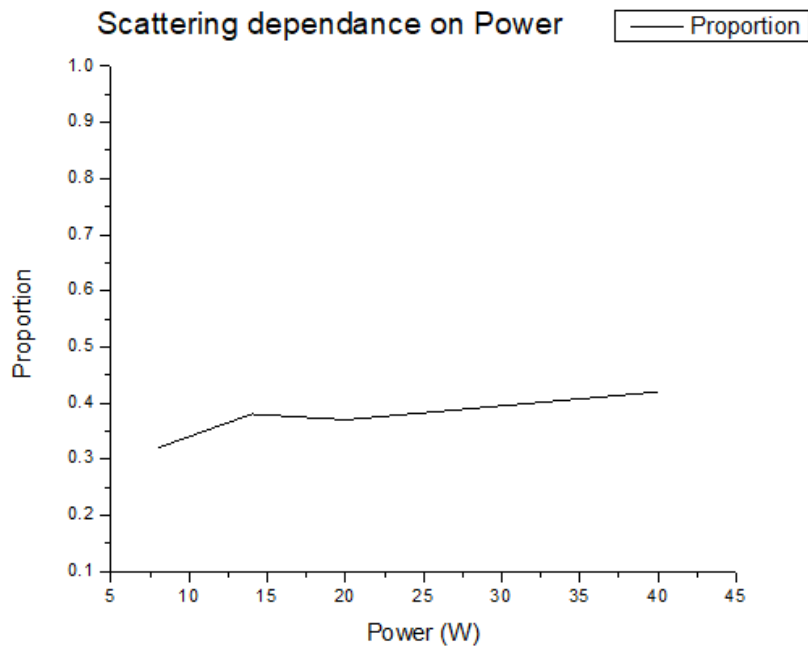

Fig. 34. Light scattering proportional comparison to ideal sample. Pulse duration 5 ps; 2 iterations; pulse repetition rate 100 kHz, distance between shot pulses 5µm. Incident beams wavelength for scattering measurement is 532 nm.

The big dependence on the light scattering values can be seen when we change distance between marking point (Fig. 35). As the marking point distance increases light scattering decreases, as smaller part of the surface are marked and contribute to the scattering losses. Not marked part of the surface don't contribute to the scattering signal. In this case RGB values decrease drastically also.
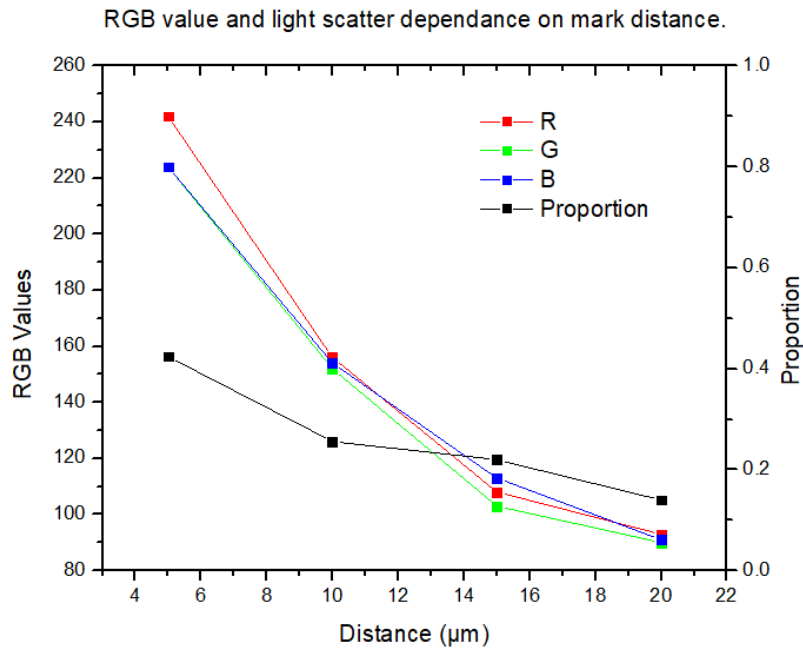
Fig. 35. Scattering light proportion and RGB values decreases as the distance between marking spots increases. Pulse duration: 10 ps, 2 iterations; pulse repetition rate 100 kHz, distance between scanning lines 5µm. Incident beams wavelength for scattering measurement is 532nm.

12.4. Best marking results.

Using Biburst mode it is possible to get white marks on the ceramics with femtosecond pulses. Lowest pulse energy to get good was about 80 µJ and most optimal parameters are show in table 4, examples of marks in Figure 36.

Nr	Pulse energy, µJ	Laser Power, W)	Biburst mode		R	G	B
			p	n			
1.	80	8	4	2	191	184	192
2.	140	14	4	2	215	204	208
3.	200	20	4	2	222	206	206
4.	140	14	2	4	208	198	199
5.	200	20	2	4	209	199	199
6.	400	40	1	4	238	222	222

Table 4. RGB values and parameters of marking of best examples made using Biburst mode. 100 kHz repetition rate, marked one time, marked one time, pulse duration 243 fs.

Fig. 36. Visual presentation of marked examples. Numbers in the picture are related to Table 3.

Other examples of best RGB values are shown in Table 5. These examples have good RGB values and used in standard laser mode. We didn't get any good contrast with pulse duration lower that 2.5 ps for standard laser mode using point by point ablation.

Nr	Pulse energy, µJ	Laser Power, W)	Space between marking spots, µm	Times of repeat.	Pulse width, ps	R	G	B
1.	80	8	5	1	2,5	203	193	194
2.	140	14	5	1	2,5	216	197	199
3.	140	14	5	1	5	217	198	191
4.	200	20	5	1	5	222	204	204
5.	140	14	5	1	10	247	228	230
6.	200	20	5	1	10	242	226	227

Table 5. Best marking results. Pulse repetition rate 100 kHz.

With point by point ablation we got 12 usable marks with high contrast and RGB values. More white marks were created when we in increased pulse overlap rate (Table 6), laser beam was scanned in line with certain space between them.

RGB values don't match white paper values, but as we mentioned RGB values are not fully correct, because of the errors which was made due poor calibration capabilities and there is possibility that white paper smooth surface reflects more light. Visually looking all examples looking white and hard to see the difference between white paper and mark whiteness.

.Nr.	Pulse energy, µJ	Pulse repetition rate, kHz	Scanning speed, mm/3	Pulse duration, ps	Programmed space between scanned lines.	R	G	B
1	36	100	100	1	5	255	255	245
2	36	100	150	1	5	255	241	240
3	36	100	100	2	5	254	248	236
4	36	100	150	2	5	253	247	235
5	36	100	100	2	10	243	236	217
6	14	251	200	1	5	252	248	239
7	14	251	300	2	5	229	223	217
8	14	251	100	1	5	241	232	217

Table 6. Best marking results, for different pulse overlap. Every sample was marked one time.

All marked marks are hydrophilic and water on them spreads a lot and then mark color changes and dims the color (Fig. 37).
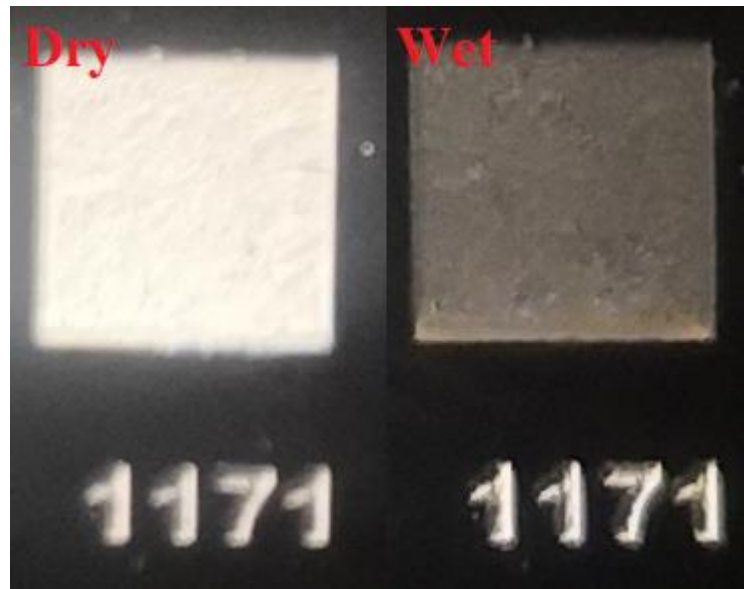
Fig. 37. Example of how color changes because mark and marked material is hydrophilic. On the right mark was moistened with water droplet. Marking parameters mentioned in Table 4, Example Nr.6

13. Analysis of laser textured surfaces for improvement of wetting properties of the surface.

To decrease hydrophilic properties of the surface I tried to fabricate periodic structures on glass ceramic based on research which I presented earlier. Two types of periodic structures were formed: micrograting structure and periodic rectangular pillar structure [41-45]. All structures were created using second harmonic wavelength, pulse repetition rate of 100 kHz and pulse energy was 14,4 µJ. Laser ablated lines were 16-19µm width. Created structures was washed in ultrasonic bath for 30 minutes. Surfaces were analyzed using microscope, profilometer. For end results contact angle with water was measured.

13.1. Surface analysis of created microgratings.

Working with our laser marking system smallest micrograting we were able to create 14 µm, 32 µm and 62 µm wide lines on the surface. For line quality and surface texture biggest impact had scanning speed. With lower scanning speed (100 mm/s) created microgratings had poor quality and was hardly recognizable. Created lines with 100 mm/s were destroyed (Fig. 38), pulse overlap accumulated more heat in the ablation area which affected material unevenly.
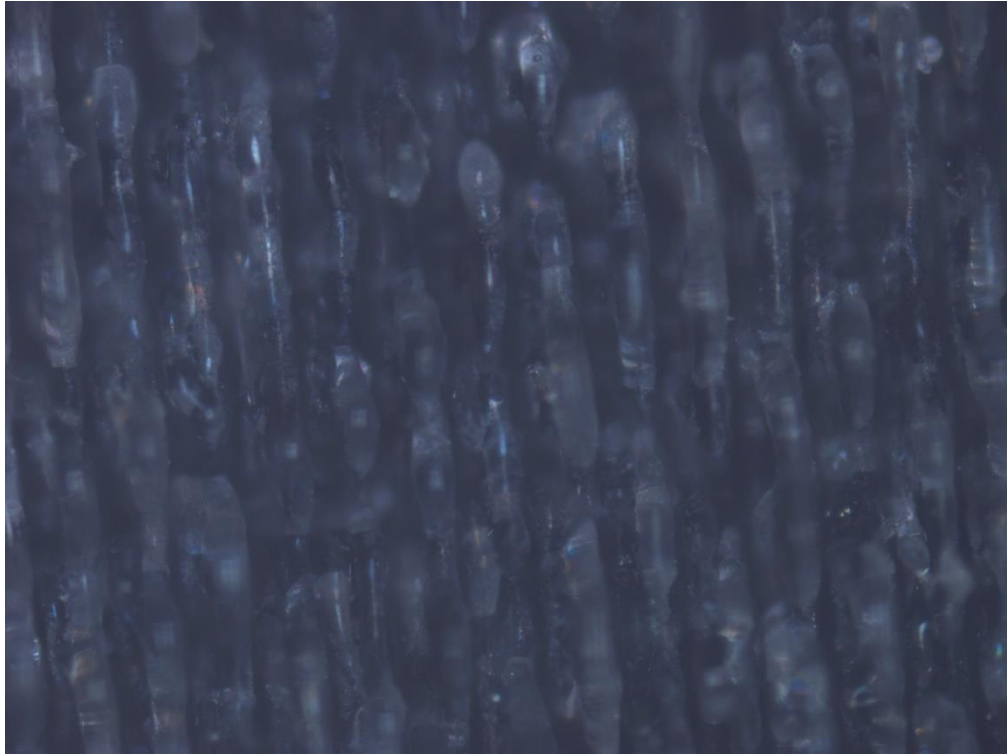
Fig. 38. Poor quality microgratings with scanning speet of 100 mm/s,

If we take a look at the surface profile (Fig. 39) it's hard to recognize where lines were created, and what line width was. Created structure is more random and not periodic at all, had some deep voids. For void generation glass-ceramic porosity and additives could also had an impact. Mechanical durability was very poor because most samples was destroyed after washing in ultrasonic bath.

With higher scanning speed we were able to create more periodic and more precise structures (Fig. 40). We were able to measure width of the gratings and space between them. Created grating with width of 14 µm was not perfect, because height of these structures was about only 6 µm. We got good sample with line width of 32 µm and height of the pillars was about 28 µm.
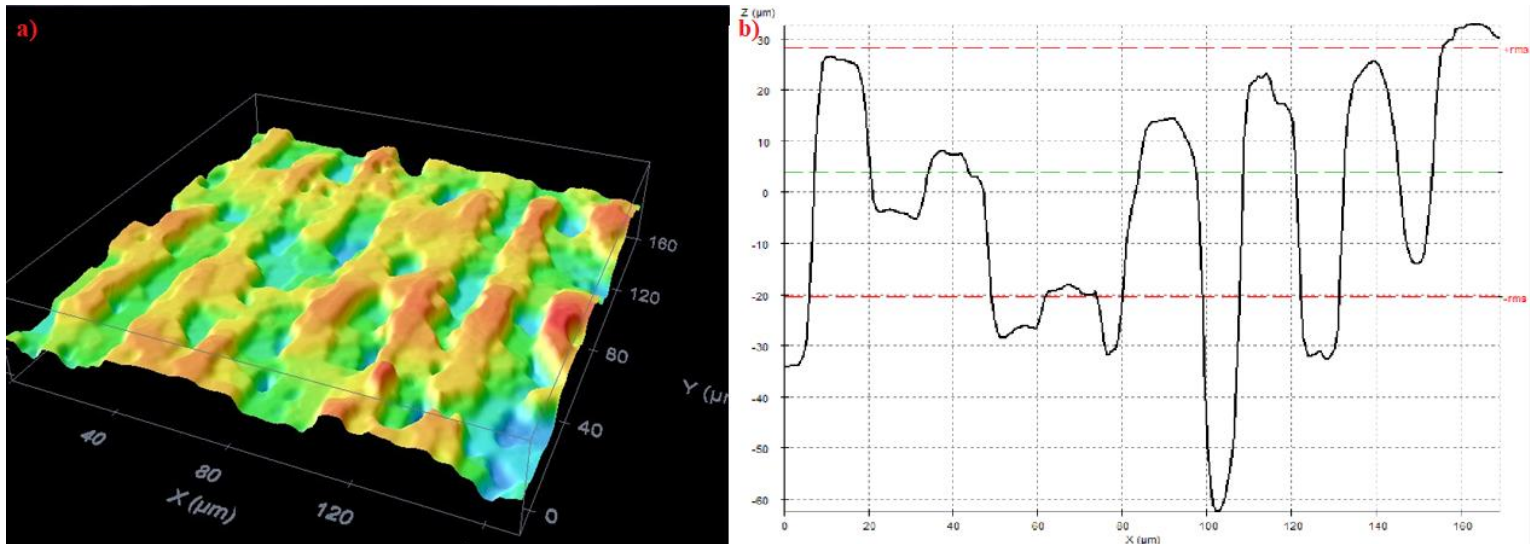

Fig. 39. Poor quality of textured sample. a) 3D profile of the surface; b) Height profile.
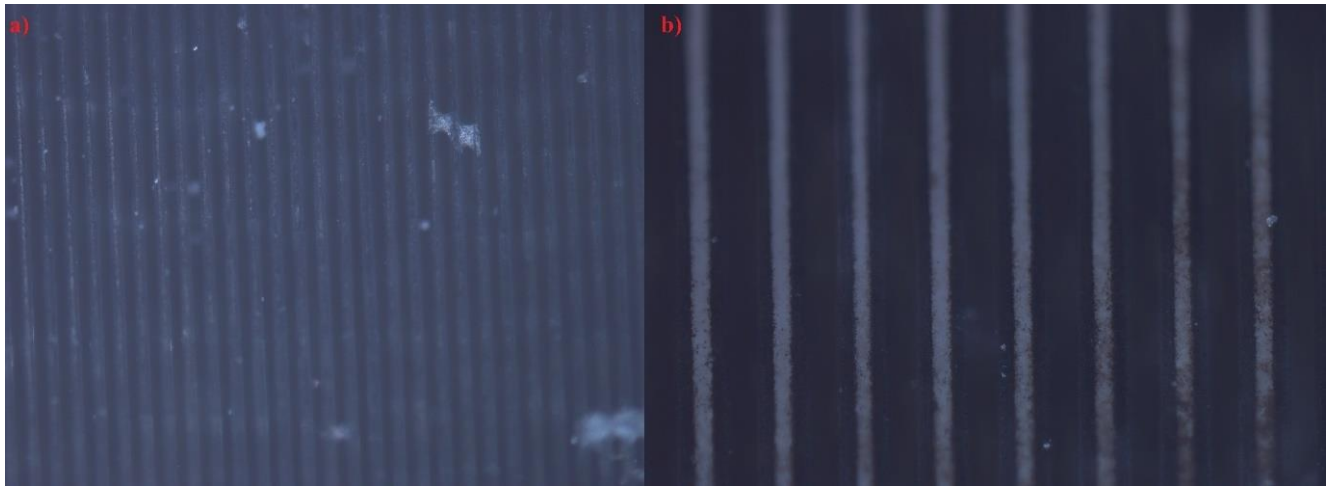
41

Fig. 40. Created microlines with scanning speed of 300 mm/s. a) 14 µm wide, 60 iterations; b) 32 µm wide 50 iterations.
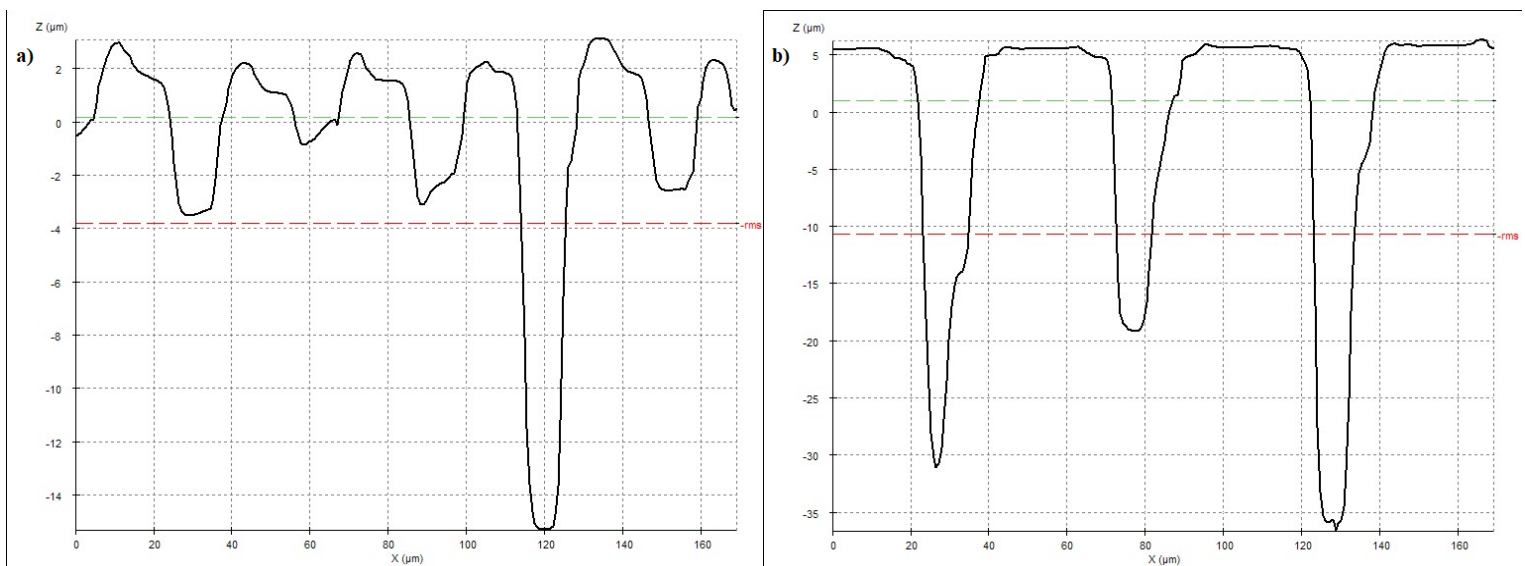

Fig. 41. Height profile of samples scanned with scanning speed of 300 mm/s. a) 14 µm wide, 60 iterations; b) 32 µm wide 50 iterations.

13.2. Surface analysis of created pillars.

Scanning speed has also had same impact as creating microripples. Most precise pillars were created using scanning speed of 200 mm/s (Fig. 42).
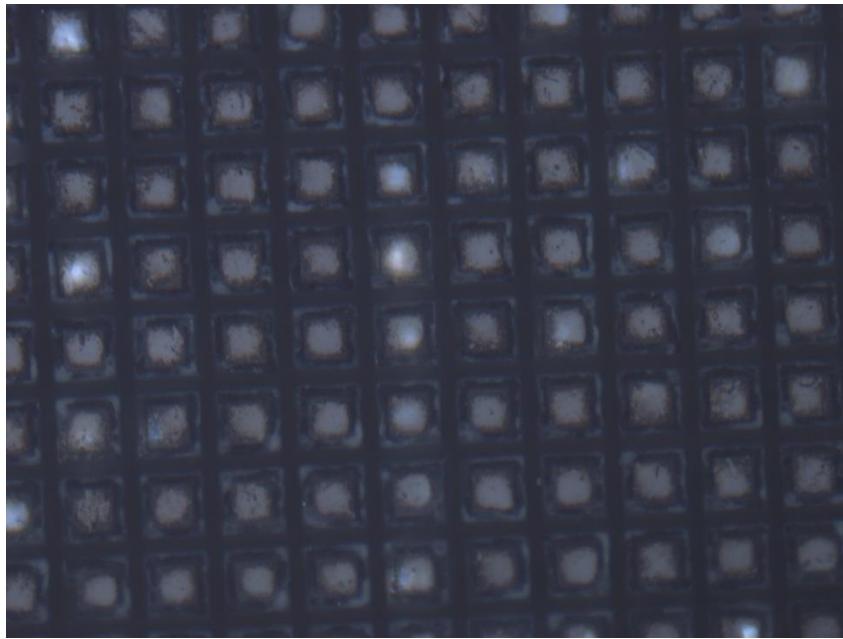
Fig 42. Marked sample with scanning speed of 200 mm/s. 40 iterations. Pillar size is 62 μm

Marking with lower scanning speed (100 mm/s) creates squares with uneven top surface and size. (Fig. 43).
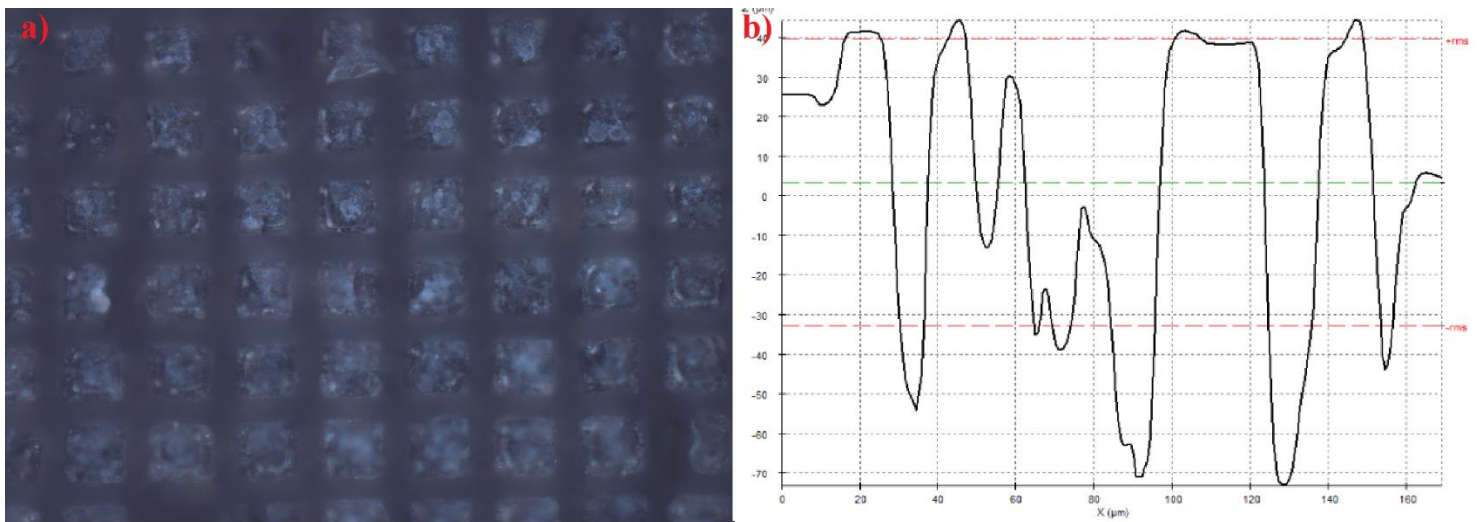

Fig. 43. a) Marked sample image view. b) Height profile of marked sample.

By increasing scanning speed ablation depth gets smaller. For example, with scanning speed of 300mm/ textured pillar height was about 10-15 µm (Fig. 44). The height of created structures is important factor, because higher pillars enhances probability to create Cassie-Baxter wetting state.
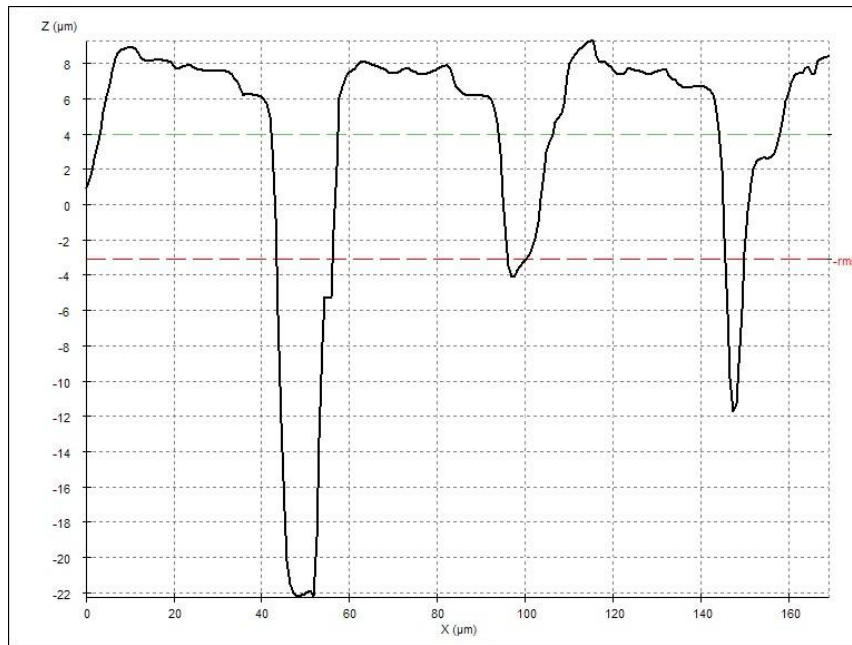
Fig. 44. Height profile of textured pillars when scanning speed was 300 mm/s, 40 iteratons, pillar size 42 µm.

One of the main disadvantages of these type of marking texture was poor mechanical durability. After ultrasonic washing all samples were affected some part of the pillars were destroyed.

13.3. Contact angle measurement.

For contact angle measurement phone camera and "Adobe photoshop 2020" software was used. 2µl of water droplets were dropped on the surface. Our glass ceramic surface is hydrophylic, contact angle with water only reaches 19,2⁰ (Fig 45). On marked material contact angle increased by a little and it was 23,5⁰ (Fig. 46). Rectangular patterned surface didn't make big change and contact angle was 20,3⁰ (Fig. 47). Biggest improvement was made creating microgrooves on the surface and contact angle with water was 28⁰ (Fig. 48).

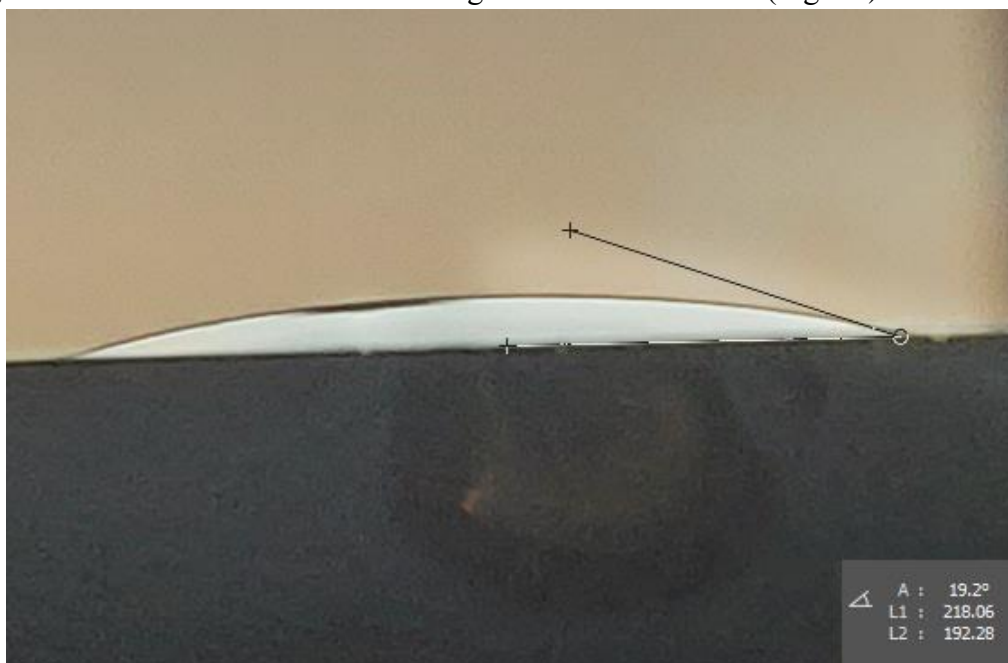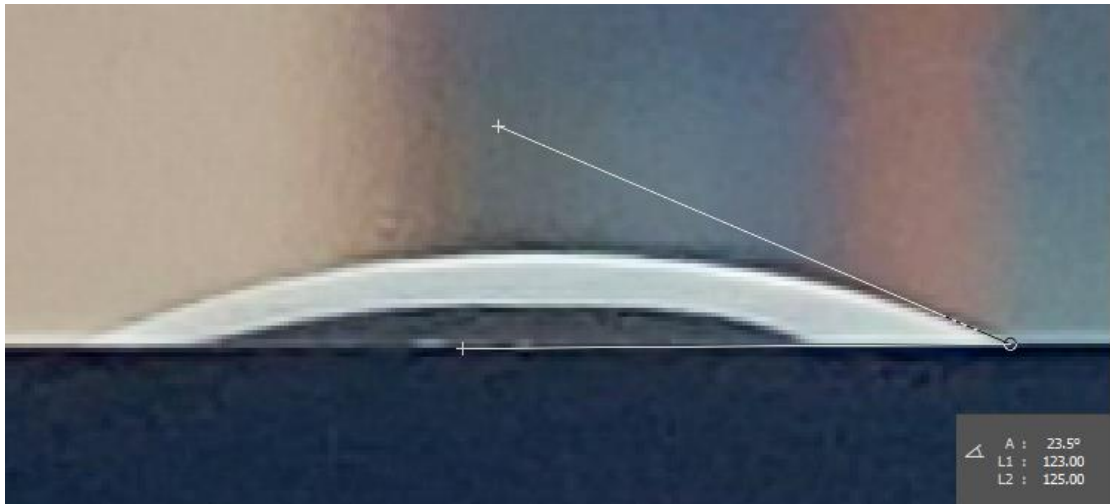Fig. 45. Water contact angle of unmarked glass-ceramic working material.

Fig. 46. Water contact angle of marked glass-ceramic working material.

Fig. 47. Water contact angle on glass-ceramic working material on textured rectangular pillars. Textured pillar size 35 µm.
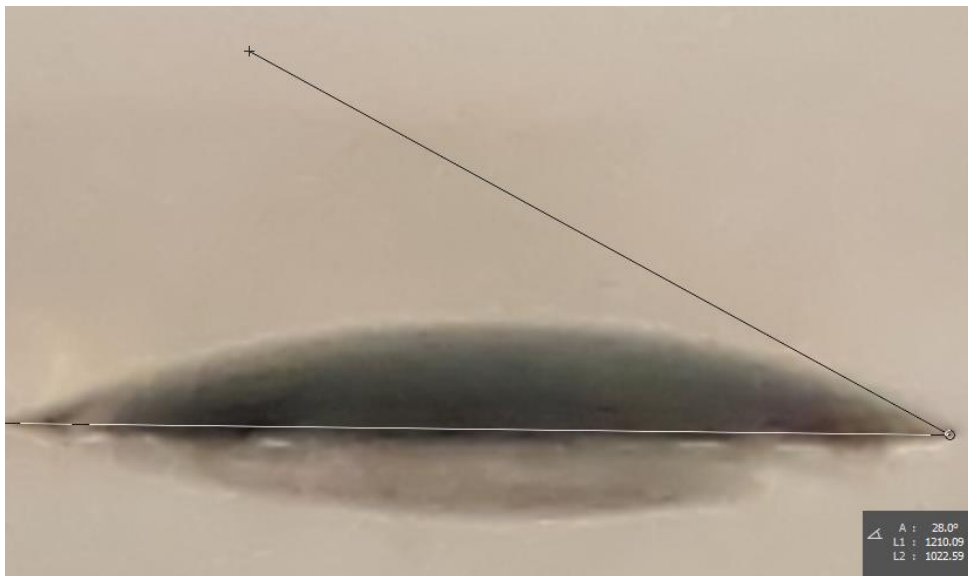
Fig. 48. Water contact angle on glass-ceramic working material on textured microgrooves. Textured microgrooves are 32 µm width.

13.4. Contact angle measurement after silanization.

After silanization we got better results, but we were not able to get hydrophobicity with pillar shaped textured surface. We were able to create hydrophobic surface for sample with created microgrooves with contact angle of 92.6º. Best contact angle values for pillar shaped texture was 69.2º.

Fig. 25. Water contact angle on glass-ceramic working material on textured and silanized microgrooves. Textured microgrooves are 24 µm width. 60 iterations. Scanning speed 300 mm/s
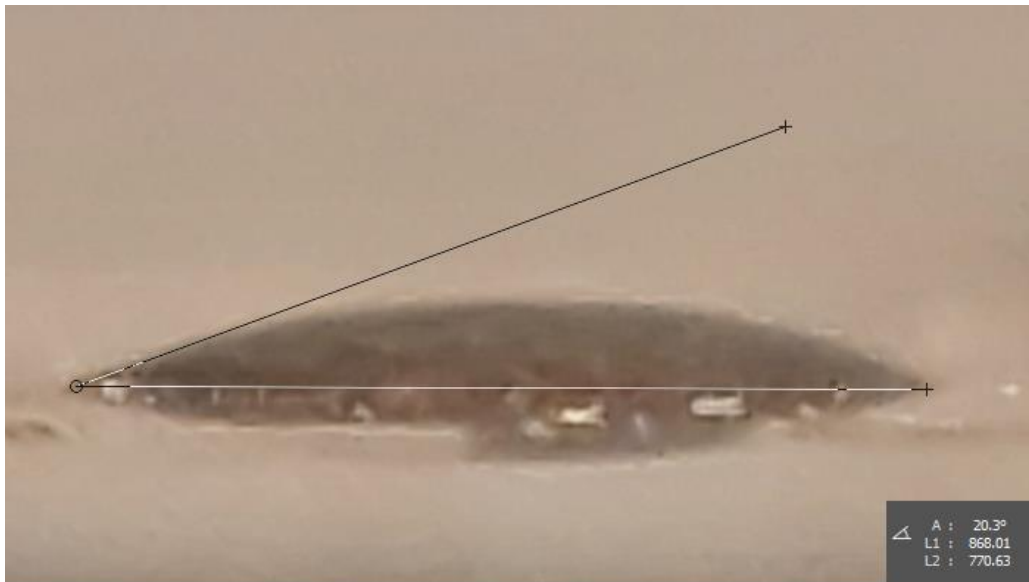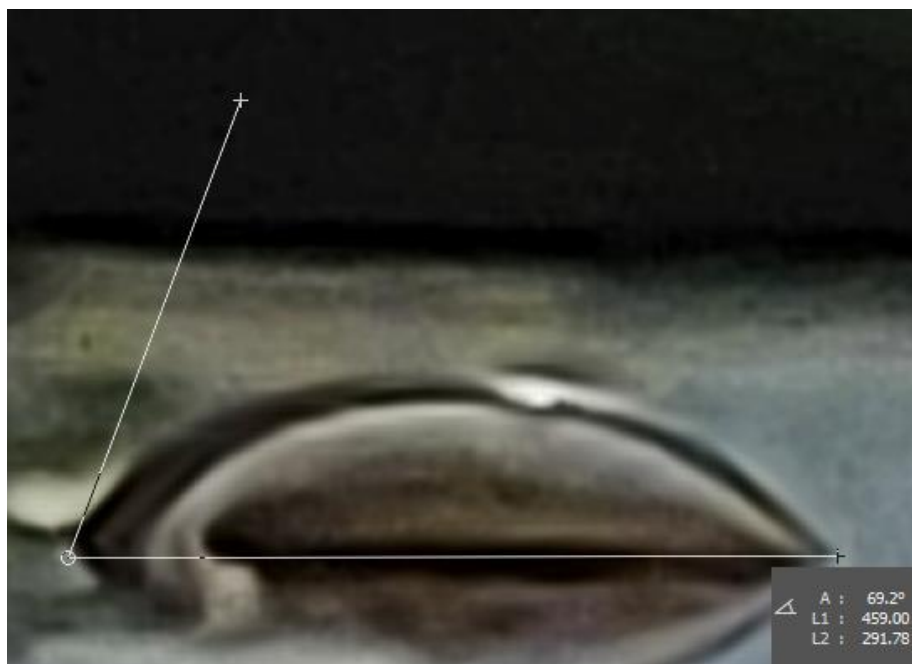

Fig. 30. Water contact angle on glass-ceramic working material on textured and silanized rectangular pillars. Textured pillar size 35 µm. 50 iterations. 300 mm/s

In the final results most our glass ceramic material surface even with laser textured patterns remained hydrophilic after silanization. One of the main reason can be that we didn't used good hydrophobic agent to coat our material after laser processing, where as in researched articles all textured surfaces were coated with fluoroalkysilane, where as we coated with hexamethyldisilazane. There is a big possibility that the difference in chemical compound had an impact on contact angle values, because fluoroalkysilane connects with the glass more efficiently and easily. Nonetheless the contact angle values after silanization increased more than three times. So silanization process was necessary to improve hydrophobicity, but it is unknown how durable silanized hydrophobic films are in house appliance environment and how it manages high temperatures.

While working with second harmonic laser power only reached 1,44 W so pulse energy was low. We could not reach pillar or groove average height more than 30µm through all laser textured area. System focused beam diameter was too wide to create smaller and more accurate structures, heat affected zone was high enough to damage created microgrooves and pillars and cause irregularities. Creating larger pillar and microgratings reduce probability of Cassie-Baxter wetting regime for inhomogenous wetting and Wenzel wetting state is not beneficial for us if we don't use hydrophobic coatings, because additional roughness in Wenzel wetting state only increases hydrophobicity of the material. While texturing and trying to reach hydrophobicity we didn't made any structures and textures which also will have good contrast Even if we would be able to create hydrophobic surfaces. We also need to investigate what marking parameters we would need to mark thin surface area of the texture and won't damage the hydrophobic microstructure, because smallest measured depth of a mark was 40 µm, which is the same depth as the highest height of our manufactured surface textures.

Conclusions.

1. Using ultrashort pulses it is possible to achieve good contrast of markings on the glass ceramic surface using surface roughness increasing by surface ablation.
2. At least 20 samples were made with good RGB values around (200:200:200) or higher changing different laser parameters: pulse energy, pulse repetition rate, pulse duration, scanning speed.
3. Heat accumulation is one of the main factors to create white marks, because most impactful parameters are closely related to it. In these range of parameters white marks were created: pulse duration (1 ps- 10 ps), pulse overlap (> 75%), biburst option (n>2,p>2, using fs pulses), laser frequency (100 kHz – 251 kHz).
4. Manufactured microgratings had biggest impact in increasing contact angle from 19.2⁰ up to 28⁰. Surface after laser texturing and formation of microgratings or rectangular shaped pillar remained hydrophilic.
5. After silanization contact angle values increases 3-4 times. Water contact angle values on the surface with rectangular pillar changed from 19.2⁰ up to 69.2⁰ and on the surface with microgratings from 28⁰ up to 92⁰.

Reference list.

1. L. YI, The advances and characteristics of high-powerdiode laser materials processing. *J. Optics and Lasers in Engineering*. **34**, 231-253 (2000).

2. I.John*, Laser Processing of Engineering Materials: Principles, Procedure and Industrial Application* , 1st edition, p. 383-390 (2005).

3. LYUBOMIR LAZOV, HRISTINA DENEVA, PAVELS NARICA, Laser Marking Methods, *Proceedings of the 10th International Scientific and Practical Conference*. **1**, 108-115 (2015)

4. https://www.marketsandmarkets.com/Market-Reports/laser-marking-market-167085735.html (checked 2020-03-18)

5. N. SHRIKRISHNA , J. UDAY, SH. DIXIT , Laser Based Manufacturing, *5th International and 26th All India Manufacturing Technology, Design and Research Conference, AIMTDR 2014*, 283-316 (2014).

6. R.M. HARRIS, Technology for Plastics. *A volume in Plastics Design Library,* p. 290-307 (1999)*.

7. C.L BELANCHE. *New techniques for the aesthetic and functional marking on polymers using laser technology*, University of Zaragoza,p. 227-238(2019). .

8. LYDIA SOBOTOVA ,MIROSLAV BADIDA Laser marking as environment technology. *Open Eng*. **7**, p. 303-316, (2017).

9. A. HAN, D. GUBENCU, Analysis of the laser marking technologies, *Nonconventional technologies review*, **4**, p.-1-6 (2008).

10. DAHOTRE, N. B., & HARIMKAR, S, Laser fabrication and machining of materials. Boston, *Springer Science & Business Media*, p. 40-63.2008

11. ONA BALACHNINAITĖ, ALGIRDAS BARGELIS, ALEKSANDR DEMETJEV, REMIGIJUS JONUŠAS, GEDIMINAS RAČIUKAITIS, VALDAS SIRUTKAITIS, *Lazerinė technologija*, Vilnius university press, Vilnius, p.161-204, (2008).

12. A.A. PELIGRADA;, E. ZHOUA, D. MORTONA, L.LI, A melt depth prediction model for quality control of laser surface glazing of inhomogeneous materials*, In Optics & Laser Technology*, **33**, p. 7-13 (2001)

13. X. ZHANG, A, J.MA, B. DING, Analysis of marking glass with different process parameters based on super-pulsed laser, *Advanced Materials Research,* **602-604**, p. 929-933 (2013) 9

14. M. KUMKARA, L. BAUERB, S. RUSSB, M. WENDELA, Comparison of different processes for separation of glass and crystals using ultra short pulsed lasers, *Proceedings of SPIE*, **8972** , p. 1-16*(2014)*

15. MINGYING SUN, URS EPPELT, SIMONE RUSS and others, Numerical analysis of laser ablation and damage in glass with multiple picosecond laser pulses, *Optics Express*, **21**, p. 7858-7867 (2013).

16. S.C.AMPBELL, F.C. DEAR, D.P. HAND, D. T. REID. Single-pulse femtosecond laser machining of glass, *J. Opt. A: Pure Appl. Opt*., **7 ,**p.162–168(2005).

17. A.A PELIGRAD, E. ZHOU, D. MORTON, L. LI ,A melt depth prediction model for quality control of laser surface glazing of inhomogeneous materials, *Optics & Laser Technology* , **33(1)**, p. 7-13 (2001).

18. S. XU, C. YAO, H. DOU An investigation on 800 nm femtosecond laser ablation of K9 glassin air and vacuum, *In Applied Surface Science*, **406**, p. 91-98 (2017).

19. M.STRAFE, A. MARCU, N.PUSCAS Pulsed laser ablation of solids, *Springer Series in Surface Sciences,* p.39-47 (2014)

20. B. GU, New laser marking technology using ultra-fast lasers, *SPIE proceedings,* **5713** (2005).

21. S. VALETTEA, E. AUDOUARDA, R. LE HARZICA, Heat affected zone in aluminum single crystals submitted to femtosecond laser irradiations, *In Applied Surface Science, 239 , p. 381-386 (2005).*

22. W. KAUTEK, J. KRUGER, Laser ablation of dielectrics with pulse durations between 20 fs and 3 ps, *Appl. Physics*, **69**, 3146 (1996).

23. V. VEKTERIS, A. KASPARAITIS, S. KIAUŠINIS, R. KANAPENAS, *Matavimu teorija ir praktika* (Žiburio leidykla, 2000).

24. J. C. STOVER, *Optical Scattering: Measurement and Analysis* (SPIE Press, Bellingham, WA, 1995), second edition.

25. R. E. HUMMEL, K. H. GUENTHER, *Handbook of Optical Properties: Thin Films for Optical Coatings* (CRC-Press, Florida, USA, 1995), 1 edition.

26. R.L SUTHERLAND, *Handbook of nonlinear optics*, Marcel Dekker Inc, 2nd edition, p. 579-590 (2003).

27. A. DUBIETIS, *Netiesinė optika*, Vilnius university, Vilnius, p. 135-140p (2011). 11

28. A. DUBIETIS, G. TAMOŠAUSKAS, A. VARANAVICIUS, AND G. VALIULIS, Two-photon absorbing properties of ultraviolet phase-matchable crystals at 264 and 211 nm, *Applied Optics* **39**, 2437–2440 (2000)

29. JR, E.K. *Principals of laser materials processing. . John Wiley & Sons, Inc,.* 837 p. (2009)

30. DIAZ, R. CHAMBONNEAU, M. GRUA, P. RULLIER, J. NATOLI, J. LAMAIGNÈRE, L. Influence of vacuum on nanosecond laser-induced surface damage morphology in fused silica at 1064 nm. *In Applied Surface Science*, **362**, p. 290-296 (2016).

31. E.D ZANOTTO, A bright future for glass-ceramics*, In ICACC' 11 & Electronic materials and applications*, p. 1-10 (2011).

32. M.H. LEWIS. *Glasses and glass-ceramics. Centre for advanced materials technology*, University of Warwick, Coventry, UK.p. 275-345 (1989).

33. W. HOLLAND, G. H BEALL. *Glass-ceramic technology*, John Wiley&Sons, New Jersey, 2nd edition (2012).

34. A. I. Berezhnoi, *Glass-Ceramics and Photo-Sitalls*, Plenum press, New York-London, 250-300 (1970).

35. T.MING, Design and fabrication of super-hydrophobic surfaces by laser micro/nano-processing, Huazhong University of Science & Technology, China, p. 17- 24 (2012).

36. N. GAO, Y. YAN, Modeling Superhydrophobic Contact Angles and Wetting Transition, *Journal of Bionic Engineering, 6 (4), p. 335-340 (2009).*

37. A. TAWFEEQ, G.K KANNARPADY, B. WRIGHT, Current Trend in Fabrication of Complex Morphologically Tunable Superhydrophobic Nano Scale Surfaces, *Applied Surface Sciences*,**384**, p. 311-332 (2016) .

38. A, MARMUR, Wetting on Hydrophobic Rough Surfaces: To Be Heterogeneous or Not To Be?, *Langmuir*, **19**, 8343-8348 (2003).

39. Ali T ABDULHUSSEIN G.K KANNARPADY, B. WRIGHT, Current Trend in Fabrication of Complex Morphologically Tunable Superhydrophobic Nano Scale Surfaces, *Applied Surface Science*, **384**, p. 311-332 (2016).

40. D. QUERE. Wetting and roughness, *Annu. Rev. Mater. Res.*, **38**:71–99 (2008).

41. J. WANG, H. CHEN, T. SUI, A. LI, D. CHEN, Investigation on hydrophobicity of lotus leaf: Experiment and theory, *Plant Science*, **176**, p. 687-695 (2009)

42. P. FAN, R. PAN, M. ZHONG, Ultrafast Laser Enabling Hierarchical Structures for Versatile Superhydrophobicity with Enhanced Cassie-Baxter Stability and Durability, *Langmuir ,* **35**, p. 16693-16711 (2019).

43. J. YONG, F. CHEN, Q. YANG, XUN HOU, Femtosecond Laser Controlling Wettability of Solid Surfaces, *Soft Matter*, **11**, p. 8897-8906 (2015).

44. SH. AHSAN, F. DEWANDA, M. SEOP LEE and others, Formation of superhydrophobic soda-lime glass surface using femtosecond laser pulses, *Appl. Surf. Sc., 265, p. 784-789 (2013).*

45. L. B. BOINOVICH, A. G. DOMANTOVSKIY, A. M. EMELYANENKO and others, Femtosecond laser treatment for the design of electro-insulating superhydrophobic coatings with enhanced wear resistance on glass., *Appl. Mater. Interfaces*, **6 (3)**, p. 2080-2085 (2014).

46. T. YANG, M. WANG, X. WANG and others, Transparent superhydrophobic solar glass prepared by fabricating groove-shaped arrays on the surface, *Soft Matter*, **16**, 3678-3685 (2020).

47. Y. LIN, J. HAN. ,M. CAI, W. LIU, X. LUO, H. ZHANG, M. ZHONG, Durable and Robust Transparent Superhydrophobic Glass Surfaces Fabricated by Femtosecond Laser with Exceptional Water Repellency and Thermostability, *J. Mater. Chem. A, 6, p. 9049-9056 (2018).*

48. H. NGUYEN, A. KIET TIEU, SH. WAN, H. ZHU, S. T. PHAM, B. JOHNSON, Surface characteristics and wettability of superhydrophobic silanizedinorganic glass coating surfaces textured with a picosecond laser, *Appl. Surf. Sc.,* **537**, 147808 (2021).

49. G. AZIMI, R. DHIMAN, H. KWON, A. T PAXSON, K. VARANASI , Hydrophobicity of rare-earth oxide ceramics, *Nat Matter*, **12**, p. 315-320 (2013).

50. A. Y. VOROBYEV, CH. GUO, Multifunctional surfaces produced by femtosecond laser pulses, *Jounal of Applied Physics,* **117**, 033103 (2015).

51. http://lightcon.com/Product/CARBIDE.html?tab=4 *(checked 2021-01-20).*

52. A. ŽEMAITIS, M. GAIDYS, P. GEČYS, M. BARKAUSKAS, M. GEDVILAS, Femtosecond laser ablation by bibursts in the MHz and GHz pulse repetition rates, *In Optics Express, 29 (5), p. 7641-7653 (2021).*

53. E. KIM, S. JANG, S. LEE, Color Correction for the Mobile Phone Camera. *Conference: Proceedings of the 2006 International Conference on Image Processing*, **1**, (2006).

54. G. HU, Shiyu FU, F. CHU, Relationship between Paper Whiteness and Color Reproduction in Inkjet Printing, *Bioresources*,**12(3)** ,p. 4854-4866 (2017).

55. L.MAZULE, S. LIUKAITYTE, R. C. ECKARDT, A. MELNINKAITIS, O. BALACHNINAITE and V. SIRUTKAITS, A system for measuring surface roughness by total integrated scattering, *Appl. Phys.*, **44**, 505103 (9pp) (2011).

Santrauka.

Darbo pagrindinis tikslas – sukurti didelio kontrasto hidrofobinius užrašus ant specialios stiklo keramikos naudojant ultratrumpuosius lazerinius impulsus. Darbe naudojama stiklo keramika dažniausiai yra naudojama indukcinių viryklių paviršiuose. Naudojamos stiklo keramikos ženklinimo pavyzdžių yra labai mažai mokslinėje literatūroje, o hidrofobinių paviršių sukūrimo pavyzdžių naudojant lazerinį ženklinimą ant tokių paviršių beveik nerasta.

Literatūros apžvalgoje yra pateikiami lazerinio ženklinimo privalumai, būdai ir kaip lazerio parametrai gali nulemti ženklinimo kontrastą, gylį ir plotį stikluose. Taip pat apžvelgta nuo ko priklauso hidrofobinių paviršių susidarymas, kas lemia hidrofobinių paviršių susiformavimą, paimti keli pavyzdžiai, pateikti gauti rezultatai, gamybos metodai ir lazerio parametrai.

Darbo metu kontrastui ir hidrofobinio paviršiaus pagaminimui buvo naudotos dvi atskiros ženklinimo sistemos, kuriose buvo įdiegti CARBIDE lazeriai iš „Light Conversion, UAB, Vilnius''. Ieškant parametrų, su kuriais gali būti sukurti tinkamo kontrasto užrašai, buvo keičiami tokie lazerio parametrai: galia, impulso trukmė, impulsų pasikartojimų dažnis ir taip pat atitinkamai keičiamas skenavimo greitis. Bandant pagaminti hidrofobinius paviršius lazerio parametrai nebuvo keičiami, tačiau buvo atsižvelgiama į skenavimo greitį ir paviršiaus struktūrų modelius.

Kontrastas buvo tiriamas matuojant raudonos, žalios ir melynos spalvų vertes. Ženklinti paviršiai ir raštai taip pat buvo tiriami naudojant mikroskopą ir profilometrą. Sukurtų paviršių hidrofobiškumas buvo analizuojamas pagal susidaranti kampą tarp vandens lašelio paviršiaus ir medžiagos paviršiaus, jiems kontaktuojant.

Tyrimų išdavoje buvo nustatyta lazerių parametrų ir skenavimo greičių verčių sritis, kurioje galima sukurti didelio kontrasto paviršius bei baltos spalvos ženklus. Ta parametrų sritis buvo pakankamai plati ir tai leido sukurti ir ištirti ~ 20 tinkamo ženklinimo pavyzdžių. Tačiau darbo metu vien lazeriniu ženklinimu nepavyko sukurti norimus hidrofobinius paviršius, visi paviršiai po lazerinio apdorojimo išliko hidrofiliniais, gautas didžiausias kampas - 28^0. Tačiau padengus medžiagą heksametildisilazanu pavyko gauti hidrofobinį paviršiu, gautas didžiausias kampas – $92,6^o$.

Summary

The main purpose of the work – create high contrast hydrophobic textures on special glass-ceramics using ultrashort pulses. In this work glass-ceramic material are mostly used for induction cooktops. There are not many marking examples of glass-ceramic material and examples of creating hydrophobic surfaces on this type of material are close to none.

In literature analysis we presented laser marking advantages, types of laser marking and how laser parameters determine marking contrast, depth and width on the glasses. Also presented what determines hydrophobic surface, howto get hydrophobic surfaces, analyzed few examples of hydrophobic surfaces on the glass, showed our results, manufacturing methods and what laser parameters were used.

In this work to get good contrast and hydrophobic surfaces we used two different marking systems which had CARBIDE laser from "Light Conversion UAB, Vilnius''. While searching for good parameters to achieve good contrast changeable parameters were laser power, pulse duration, pulse repetition rate and scanning speed. Laser parameters was not changed manufacturing hydrophobic surfaces, but we were changing scanning speed, texture types and models.

Contrast was analyzed measuring red, green, blue colour values. Marked surfaces and marks also was analyzed using microscope and profilometer. Hydrophobicity of created structures was analyzed measuring contact angle between water droplet surface and material surface when laser droplet lands on the surface.

In conclusion of our research laser parameters and scanning speed values are mentioned, where we were able to get white marks with good contrast. There were wide range of good laser parameters to get white marks with good contrast and we presented and researched 20 good mark examples. Using only laser texturing we were not able to get hydrophobic surfaces and all laser textured surfaces remained hydrophilic, highest contact angle was 28º. However when surface was coated with hexamethyldisilazane, contact angle increased and hydrophobic surface was made with contact angle of 92,6º.